Conodont zones and related ash beds through the Permian-Triassic Boundary in South China

Ning Zhang, Wenchen Xia*, Qinglai Feng, Qiuling Gao, Wenli Zhong and Sha Wu
State Key Laboratory of Biogeology and Environmental Geology, China University of Geosciences, Wuhan, 430074, China
*Corresponding author: xiawch@cug.edu.cn

ABSTRACT: Six sections from diverse paleogeographic settings in South China provide a high-resolution succession of conodont zones and associated ash beds through the Permian-Triassic boundary. A complete succession of eight conodont zones and eight associated ash beds is recorded in the basin-filling sequences: in ascending order, the *Clarkina yini* Zone with top ash bed 1, the *Clarkina meishanensis* Zone and ash bed 2 within it, the *Clarkina taylorae* Zone with ash bed 3 at its base, the *H. changxingensis*-*C. microcuspidata* Zone with ash bed 4 at its base and ash bed 5 within it, the *Hindeodus parvus* Zone with top ash bed 6, the *Isarcisella staeschei* Zone and ash bed 7 within it, the *Isarcisella isarcica* Zone and ash bed 8 within it, and the *Neogondolella krystyni* Zone. In slope settings, ash bed 3 and the *C. taylorae* Zone are missing; whereas in the strata of the platform interior, the *C. meishanensis* Zone and associated ash beds 1 and 2 are also missing. This pattern indicates an unconformity that represents increasing missing section in increasingly shallower deposits. The Global Stratotype Section and Point for the base of the Triassic, at Meishan, China, is recognized as having been formed in a slope setting, with an unconformity at the base of Bed 25. The identification of these conodont zones in Iran indicates their applicability outside of South China.

Keywords: conodont zones, ash beds, Permian-Triassic boundary, high-resolution stratigraphy, South China

INTRODUCTION

The Permian-Triassic boundary (PTB) is defined at its Global Stratotype Section and Point (GSSP) at the base of Bed 27c in the Meishan section, southern China. The correlation event is the first appearance (FA) of *Hindeodus parvus* (Kozur and Pjatakova 1976) in the evolutionary lineage from *H. praeparvus (H. latidentatus*) to *H. parvus* (Yin et al. 2001). Following this definition, many results from studies of the Permian-Triassic mass extinction have been documented, such as the recognition of the chief extinction event at Bed 25 in the Meishan section (Jin et al. 2000) and measurements of the numerical ages of major extinction events at 251.4±0.3 Ma (Bowring et al. 1998), at 252.6±0.2 Ma (Mundil et al. 2004) and at 252.28±0.02 Ma (Shen et al. 2011). The PTB was also recognized in endemic sections by the FA of *H. parvus* (Lehrmann et al. 1999, 2003; Nicoll et al. 2002; Metcalfe and Nicoll 2007; Ji et al. 2007; Chen et al. 2008; 2009; Jiang et al. 2011). The conodont zonation of the Meishan global stratotype section has been re-examined by Jiang et al. (2007), Metcalfe and Isozaki (2009), Metcalfe et al. (2007), and Zhang et al. (2007, 2009). Although there have been many achievements in past decades, the pattern and cause of end-Permian extinction are still debated (Xie et al. 2005; Yin et al. 2007; Chen, Benton 2012). A pivotal problem might be that the conodont and event stratigraphies of the uppermost Permian are unclear in the Meishan stratotype section.

To clarify the situation, this work attempts to document the spatial arrangement of global conodont zones and related ash beds through the PTB in several sections located in diverse paleogeographic settings in South China (text-fig. 1).

LOCATION AND STRATIGRAPHY

In addition to documented sections that were studied in relation to the conodont succession through the PTB in the past three decades (Zhao et al. 1981; Yin et al. 2001; Zhang et al. 1995, 2007, 2009; Wang 1995; Nicoll et al. 2002; Jiang et al. 2007; Metcalfe and Nicoll 2007; Ji et al. 2007; Chen et al. 2008, 2009; Wu et al. 1988; Zhu et al. 1999; Lehrmann et al. 1999, 2003; Wang and Xia 2004), six sections were examined for their conodont succession and sedimentary architecture. They are the Xinmin section in central Guizhou Province, the Zunyi section in northern Guizhou Province, the Liangfengya section in Chongqing City, the Huaying section in northeastern Sichuan Province, and the Jianshi and Xiakou sections in western Hubei Province (text-fig. 1). The conodont specimens on which this work is based were recovered from these six sections.

Five geographical domains can be proposed for detailed comparison of conodont zones and the biosedimentary features among the study sections and documented sections in South China in the Permian-Triassic transition, including the mid-upper Yangtze-Cathaysian platform interior, a northern and a southern slope, the Qinling-adjacent Basin (QAB), and the Nanpanjiang Basin (text-fig. 1). Of the six study sections, the Xinmin section is located in the Nanpanjiang Basin, the Zunyi section in the southern slope, the Liangfengya section in the platform interior, the Huaying section in north margin slope of Yangtze platform and the Jianshi and Xiakou sections in the QAB (text-fig. 1). Because a eustatic sea level fall occurred during the end-Permian (Hallam et al. 1983), differences in the conodont ranges and biosedimentary features among the six study sections can be expected (see next section).

Generally, the marine Permian-Triassic boundary interval consists of a lower and an upper lithostratigraphic complex in South China. The lower one comprises the Changxing Formation in carbonate platform interior to slope settings and the Dalong Formation in basin settings and generally appears as a rimmed carbonate platform system. The upper complex, however, consists of Yinkeng, Daye, Feixianguan, Luolou, and other local formations, and the spatial variation of biosedimentary features indi-

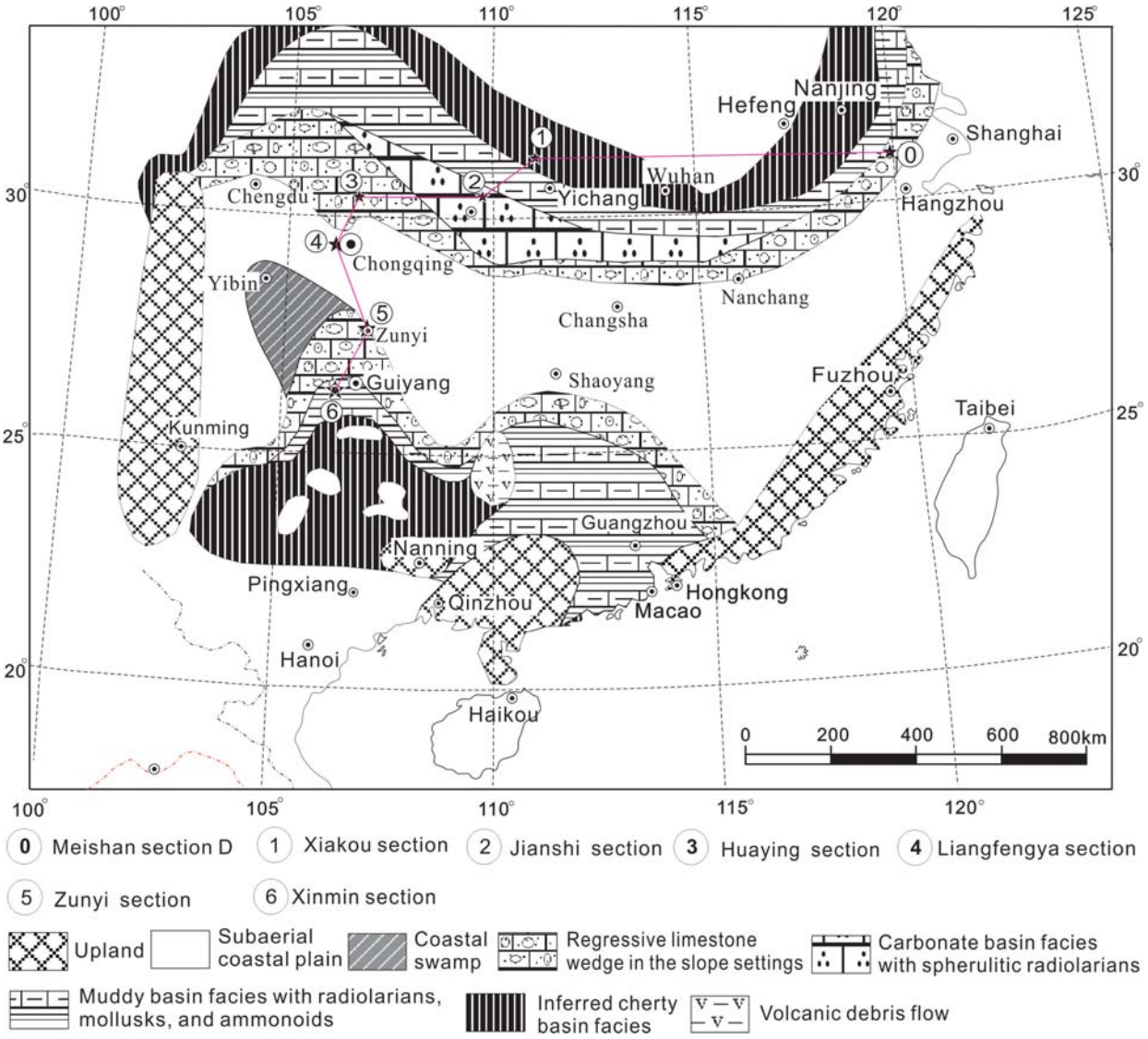

TEXT-FIGURE 1
Paleogeographic map of South China in the *C. meishanensis* conodont zone, showing the facies relationships of regressive rimmed carbonate platform system and the locations and paleogeographic settings of six study sections and documented sections.

cate a homoclinal carbonate ramp system. This paper will focus on the discussion of the geographic impact on conodont succession and related ash beds through the PTB.

Conodont Zones through the PTB

High-resolution conodont successions were calibrated through the PTB based on the detailed correlation of conodont ranges among six sections in diverse geographic settings in South China. In this succession, eight conodont zones were demarcated and are respectively described in ascending order as follows (text-fig. 2):

***Clarkina yini* Interval Zone**

Materials: This zone was recognized in the specimens from the samples Xk-246 and 248 in Xiakou section (text-fig. 3), from the samples Xm 3-2 and 3-3 in Xinmin section (text-fig. 4), from the samples Zy1 and 2 in Zunyi section (text-fig. 2), from the samples Lfy 1 and 2 in Liangfengya section (text-fig. 5), from the sample Js 115 in Jianshi section (text-fig. 2), and from the samples Hy 2, 4, 6, and 8 in Huaying section (text-fig. 2).

Description: The lower limit is marked by the first appearance (FA) of *C. yini* (Mei, Zhang and Wardlaw 1998), whereas the upper limit is marked by the FA of *C. meishanensis* in the basin- and slope-filling sequences in South China. In the strata of the platform interior, the upper limit is usually an unconformity. In addition to the index species (*C. yini*; text-fig. 6.1-6. 6), this zone also yields *C. changxingensis* (Wang and Wang 1981; text-fig. 6.7-6-10), *C. zhejiangensis* (text-fig. 6. 13-6.14), *C. tulongensis* (Tian 1982; text-fig. 6. 11), and *C. postwangi* (Tian 1993; text-fig. 6.12). In the strata of the platform interior, some specimens of *H. typicalis* (Sweet 1970) are present as well, but this species is rare in the basin-filling sequences.

Occurrence: This is a widespread biozone that universally occurs in South China (text-fig. 2 and 7). Usually there is the ash

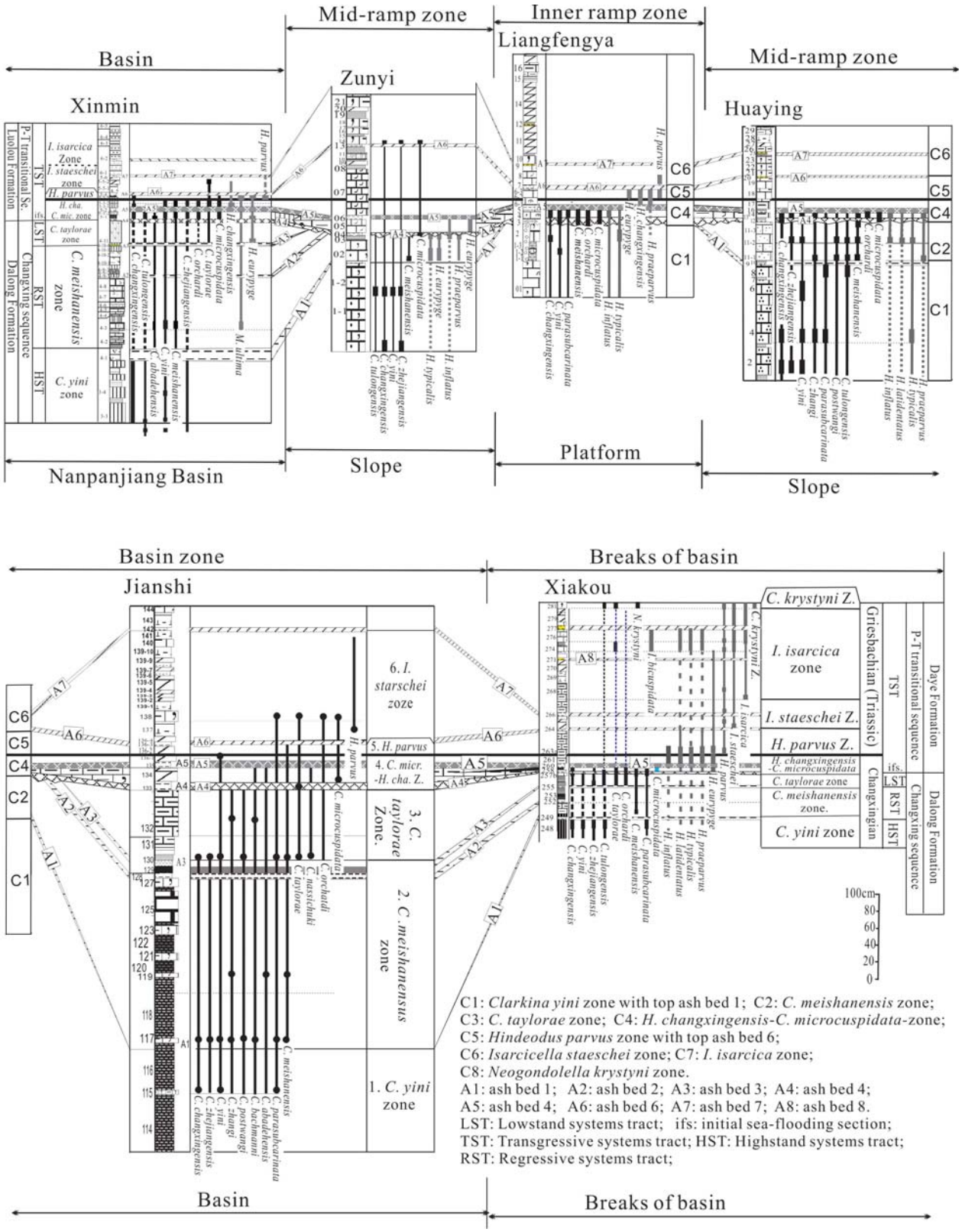

TEXT-FIGURE 2
Comparison of conodont stratigraphic ranges across the PTB throughout the Xinmin, Zunyi, Liangfengya, Huaying, Jianshi, and Xiakou sections showing geographical variation of conodont succession: in the basin-filling sequences (Xinmin, Jianshi, and Xiakou sections), there is a complete succession that consists of *C. yini* Zone, *C. meishanensis* Zone, *C. taylorae* Zone, *H. changxingensis-C. microcuspidata* Zone, *H. parvus* Zone, *I. staeschei* Zone, *I. isarcica* Zone, and *N. krystyni* Zone in ascending order; in the slope-filling sequence the *C. taylorae* zone is absent by unconformitiy; in the strata of the platform interior, the *C. meishanensis* zone is also absent.

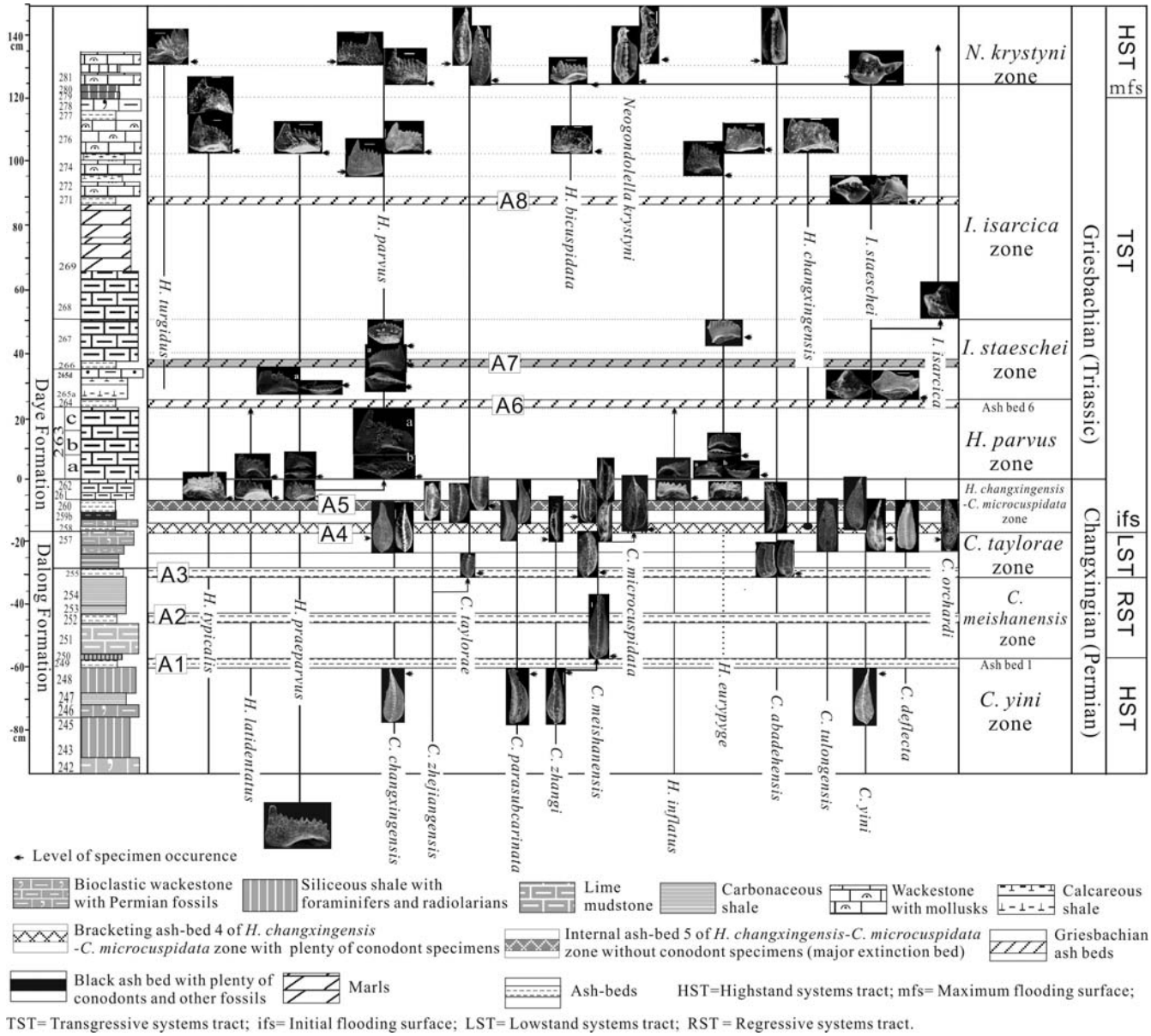

TEXT-FIGURE 3

Vertical distribution of conodont specimens through PTB in the Xiakou section (Qinling-adjacent basin) showing a columnar succession of conodont zones and related ash beds in the basin-filling sequences including, in ascending order, the *C. yini* Zone with ash bed 1 at its top, the *C. meishanensis* Zone and internal ash bed 2, the *C. taylorae* Zone with ash bed 3 at its base, the *H. changxingensis-C. microcuspidata* Zone with basal ash bed 4 and internal ash bed 5, the *H. parvus* Zone with ash bed 6 at its top, the *I. staeschei* Zone and internal ash bed 7, the *I. isarcica* Zone and internal ash bed 8, and *N. krystyni* Zone.

bed 1 at the top of this interval zone. The ash bed 1 and the upper limit of the interval zone may be truncated by unconformity in the strata of the platform interior (text-fig. 2 and 5).

***Clarkina meishanensis* Interval Zone**

Materials: This zone was distinguished in the specimens from the samples Xk 250, 251, and 254 in the Xiakou section (text-fig. 3), from the samples Xm 4-3 and 4-9 in the Xinmin section (text-fig. 4), from the sample Zy 2 in the Zunyi section (text-fig. 2), from the samples Hy11-1, 11-2, and 11-3 in the Huaying section (text-fig. 2), from the samples 24e-l and 24e-u in the Meishan section E (text-fig. 8), with the lowermost occurrence of the index species (*C. meishanensis*) in correlative sections.

Description: The interval between the FA of *C. meishanensis* (text-fig. 6. 15- 6.16, 6.18-6.23) and the FA of *C. taylorae* (Orchard 1994) is recognized as a *C. meishanensis* zone. In addition to index species (text-fig. 6. 15-6.24), this interval also contains the specimens of *C. abadehensis* (Kozur 2004), *C. yini* (text-fig. 6. 28), *C. tulongensis* (Tain 1982), *C. changxingensis* (text-fig. 6. 25-6.27), *C. parasubcaranata* (Mei, Zhang and Wardlaw 1998), *C. postwangi*, *C. deflecta* (text-fig. 6. 29), *C. zhejiangensis* (Mei 1996; text-fig, 6. 14), *C. nassichuki* (Orchard 1998), and *C. zhangi*. Many specimens of *H. typicalis* (text-fig. 6.32), *H. latidentatus* (Kozur, Mostler and Ranhimi-Yazd 1975; text-fig. 6. 31), *H. inflatus* (Nicoll, Metcalfe and Wang 2002), *H. praeparvus* (text-fig. 6. 33), *H.*

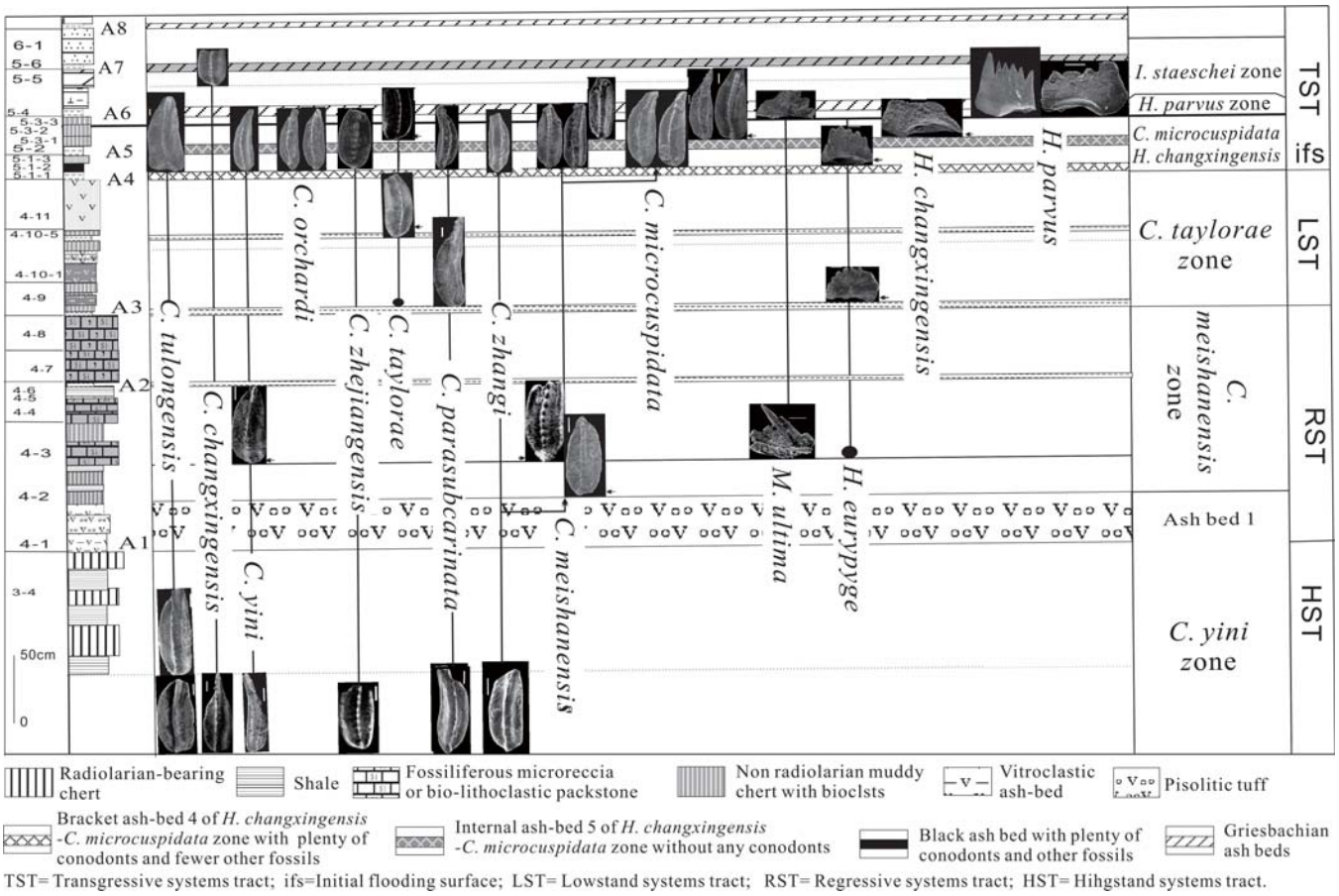

TEXT-FIGURE 4
Vertical distribution of conodont specimens through the PTB in the Xinmin section (Nanpanjiang basin) showing a columnar succession of conodont zones and related ash beds in the basin-filling sequences.

eurypyge (Nicoll, Metcalfe and Wang; text-fig, 6-30), and *M. ultima* (Kozur 2004; text-fig. 4) also appear in this zone.

Occurrence: Even though this is a widespread conodont zone, it only occurs in the slope- and basin-filling sequences in South China. In the platform interior, it is usually absent due to unconformity (text-figs. 5 and 7). In addition, ash bed 1 typically underlies this conodont zone, and the internal ash bed 2 occurs within it.

***Clarkina taylorae* Interval Zone**

Materials: This zone was recognized in the specimens from the samples Xk 256 and 257 in Xiakou section (text-fig. 3), from the sample 130 in Jianshi section (text-fig. 2), and from samples Xm 4-10-5 and 4-11-1 in Xinmin section (text-fig. 4).

Description: The interval between the FA of *C. taylorae* (text-fig. 9.2-9.4) and the FA of *H. changxingensis* and/or *C. microcuspidata* n. sp. was defined as a *C. taylorae* interval Zone in the Xiakou, Janshi and Ximin sectons, that corresponds to the *C. taylorae-C. zhejiangensis-C. yini* zone from the Chaotan section (Ji, et al. 2007). In addition to the index species (text-fig. 9.1-9.4), this interval also contains specimens of *C. meishanensis* (text-fig, 9.5-9.6), *C. changxingensis* (text-fig. 9.8), *C. parasubcarinata* (text-fig. 9. 10), *C. abadehensis* (text-fig. 9. 9), and *C. nassichuki* (text-fig. 9.7).

Occurrence: This conodont zone has ash bed 3 at its base and occurs only in basin-filling sequences in South China (text-figs. 2, 3, 4). In the strata of the slope and platform interior, it is typically missing due to a subaerial unconformity (text-fig. 7). Thus, this conodont zone was a deposited during the sea level lowstand when the shoreline was at maximum progradation.

***Hindeodus changxingensis-Clarkina microcuspidata* Interval Zone**

Materials: This zone was recognized in the specimens from the sample Xk 258, 259, 260 and 262 in Xiakou section (text-fig. 3), from the sample Js 134 in Jianshi section (text-fig. 2), from the sample Hy13 in Huaying section (text-fig. 2), from the samples Xm 5-1-2 and 5-3-1 from the Xinmin section (text-fig. 4), from the samples Lfy 3-2, 4-1, 4-2, and 6-1 in Liangfengya section (text-fig. 5), and from sample Zy 5 in Zunyi section (text-fig. 2), with the lowermost occurrence of index species (*C. microcuspidata*) in every section.

Description: The interval that begins with the FA of *H. changxingensis* (text-fig. 9.26) and/or *C. microcuspidata* n. sp. (text-fig. 9.11-9.12, 9-14, 9-18-9-19) and ends with the FA of *H.*

parvus is regarded as a *H. changxingensis-C. microcuspidata* zone. In addition to index species (text-figs. 9.11-9.19), this interval also contains the specimens of *C. meishanensis* (text-fig. 9.21-9.24), *C. yini* (text-fig. 8.27), *C. orchardi* (text-fig. 9.31), *C. parasubcarinata* (text-fig. 9.28-9.29), *C. changxingensis* (text-fig. 9.25), *C. taylorae* (text-fig. 9.32-9.33), and *C. zhejiangensis* (text-fig. 9.30). Specimens of the genus *Hindeodus* abruptly increase in this conodont zone. Common species include *H. latidentatus* (text-fig. 9.36), *H. praeparvus* (text-fig. 8. 38), *H. eurypyge* (text-fig. 9.34, 9.35), *H. inflatus* (text-fig. 8.37), and *H. typicalis* (Sweet, 1970) (Kuzor, Mostler and Rahimi-Yazd, 1975) (text-figs. 3 and 4). Statistical information indicates that the abundance and diversity of the genus *Clarkina* peaks in the lower part of this zone, whereas those of the genus *Hindeodus* peak in the upper part of this zone. Major extinctions appear exactly at the level between the lower and upper parts.

Occurrence: Both text-fig. 2 and text-fig 7 show that the *H. changxingensis-C. microcuspidata* conodont zone is widespread in South China. It typically starts with regional ash bed 4 and contains ash bed 5 in the middle. Ash bed 4 immediately rests on the *C. taylorae* zone in the basin-filling sequences and overlaps on subaerial unconformity in the strata of slope and platform interior. Thus, it was a response to an initial sea-flooding event. In summary, the *H. changxingensis-C. microcuspidata* conodont zone is restricted to a very thin but geographically widespread stratigraphic interval that can be regarded as a marker horizon for identifying the upper limit of the Changhsingian Stage. Within the Meishan global stratotype section, this conodont zone can be correlated to Bed 26 by the appearance of *H. changxingensis* (Jiang et al. 2007; Metcalfe et al. 2009). The *C. taylorae* Zone is clearly absent due to subaerial unconformitiy here (text-figs. 7 and 8). Although the first specimens of *H. changxingensis* could not be found in any sections, its coexistent specimens (*C. microcuspidata*) were universally recovered from every section in South China. Thus, we adopt the nomenclature of *H. changxingensis-C. microcuspidata* zone for this biozone.

***Hindeodus parvus* Interval Zone**

Materials: This zone was recognized in the specimens from the samples Xk-263a and 263c in Xiakou section (text-fig. 3), from the sample Xm-5-3-3in Xinmin section (text-fig. 4), and from the sample Lfy-6-2 in Liangfengya section (text-fig. 5), with the lowermost occurrence of index species (*H. parvus*) in the correlative section.

Description: The lower limit is marked by a first appearance (FA) of *H. parvus* (text-fig. 10. 1a, b, 10. 2-10.6), and the upper limit is determined by the FA of *I. staeschei* (Dai and Zhang 1989). In addition to index species (*H. parvus*), this zone also yields *H. changxingensis* (text-fig. 10.11), *H. latidentatus* (text-fig. 10.7a, b), *H. eurypyge* (text-fig. 10.10a, b), *H. inflatus* (text-fig. 10. 8a, b, 10. 20), *H. praeparvus* (text-fig. 10.9a, b) and *M. ultima* (text-fig. 4).

Remarks: It has been generally accepted that the PTB is marked by the FA of *H. parvus* (Kozur and Pjatakoa 1996; Yin et al. 2001; Ji et al. 2007; Chen et al. 2008). Early forms of *H. parvus* are difficult to distinguish from more evolved specimens on morphology in any section. Regional studies of conodont biozones and ash beds can be useful.

Occurrence: The *H. parvus* conodont zone immediately rests on the *H. changxingensis-C. microcuspidata* zone (text-fig. 2 and 7) and universally extends in South China. There is ash bed 6 At the top of this interval zone.

***Isarcicella staeschei* Interval Zone**

Materials: This zone was recognized in the specimens from samples Xk265a, 265c, and 267 in Xiakou section (text-fig. 3), and from the sample Zy 14 in Zunyi section (text-fig. 2), with the lowermost occurrence of index species (*I. staeschei*).

Description: The lower limit is marked by the FA of *I. staeschei* (text-fig. 10.12, 10.13), and the upper limit is marked by the FA of *I. isarcica* (Huckriede 1958). In addition to the index species (*I. staeschei*), this interval also contains evolved specimens of *H. parvus* (text-fig. 10.14a, b, 10.17, 10.18), *H. eurypyge* (text-fig. 10.16a, b, 19), and *H. praeparvus* (text-fig. 10.15a, b). There are also, though fewer in number, specimens of *C. changxingensis* (text-fig. 10.21, 10.24), *C. zhejiangensis* (text-fig. 10.22) and *C. microcuspidata* (text-fig. 10.23) that were recovered from the lower portion of this zone.

Occurrence: This conodont zone is underlain by ash bed 6 and usually can be subdivided into a lower and an upper interval by internal ash bed 7, which is able to be correlated with Bed 28 in the Xiakou section (text-fig. 7). Below this internal ash bed, specimens of *Hindeodus* and *Clarkina* have been recovered (text-fig. 2), whereas above it no specimens of *Clarkina* have been found so far.

***Isarcicella isarcica* Interval Zone**

Materials: This zone was recognized in the specimens from the samples Xk 268, 271, 274 and 276 in Xiakou section with the lowermost occurrence of index species (*I. isarcica*) (text-fig. 3).

Description: The lower limit is marked by the FA of *I. isarcica* at the base of bed 268 in the Xiakou section and the upper limit is affirmed by the FA of *Neogondolella krystyni* (Orchard 1998). This conodont zone can be subdivided into two intervals by ash bed 8 in South China. In the lower part, there are few conodont specimens, except the first specimen of *I. isarcica* (text-fig. 11. 1). Near the upper part, however, abundant specimens of *H. parvus* (text-fig. 11. 3-11.6), *H. praeparvus* (text-fig. 11.10), *H. eurypyge* (text-fig. 11.8, 11.9), *H. changxingensis* (text-fig. 11.11), *H. typicalis* (text-fig. 11.7), *H. bicuspidate* Kozur 2004 (text-fig. 11. 17), and *I. staeschei* (text-fig. 11. 2a, b) have been observed, whereas fewer specimens of *C. taylorae* were found.

Occurrence: This conodont zone has been recognized in the Xiakou (text-fig. 3) and Meishan global stratotype section (Zhang et al. 2009) by the FA of *I. isarcica*. It can be also subdivided into two intervals by internal ash bed 8 in South China. The lower interval contains few conodont specimens except the first specimen of *I. isarcica* (text-fig. 11.1), whereas the upper interval contains abundant specimens in the genera *Hindeodus*, *Isarcicella*, and *Clarkina* (text-fig. 3).

***Neogondolella krystyni* Interval Zone**

Materials: This conodont zone was recognized in the specimens from the samples Xk 281 and 283 in Xiakou section with the lowermost occurrence of index species (*N. krystyni*) (text-fig. 3).

Description: The lower limit is marked by the FA of *N. krystyni* (text-fig. 11.21-11.22) at the base of bed 281 in the Xiakou section, and the upper limit has not been identified in the Xiakou section. In addition to the index species, this zone also has yielded plenty of specimens of *H. parvus* (text-fig. 11. 12-11.

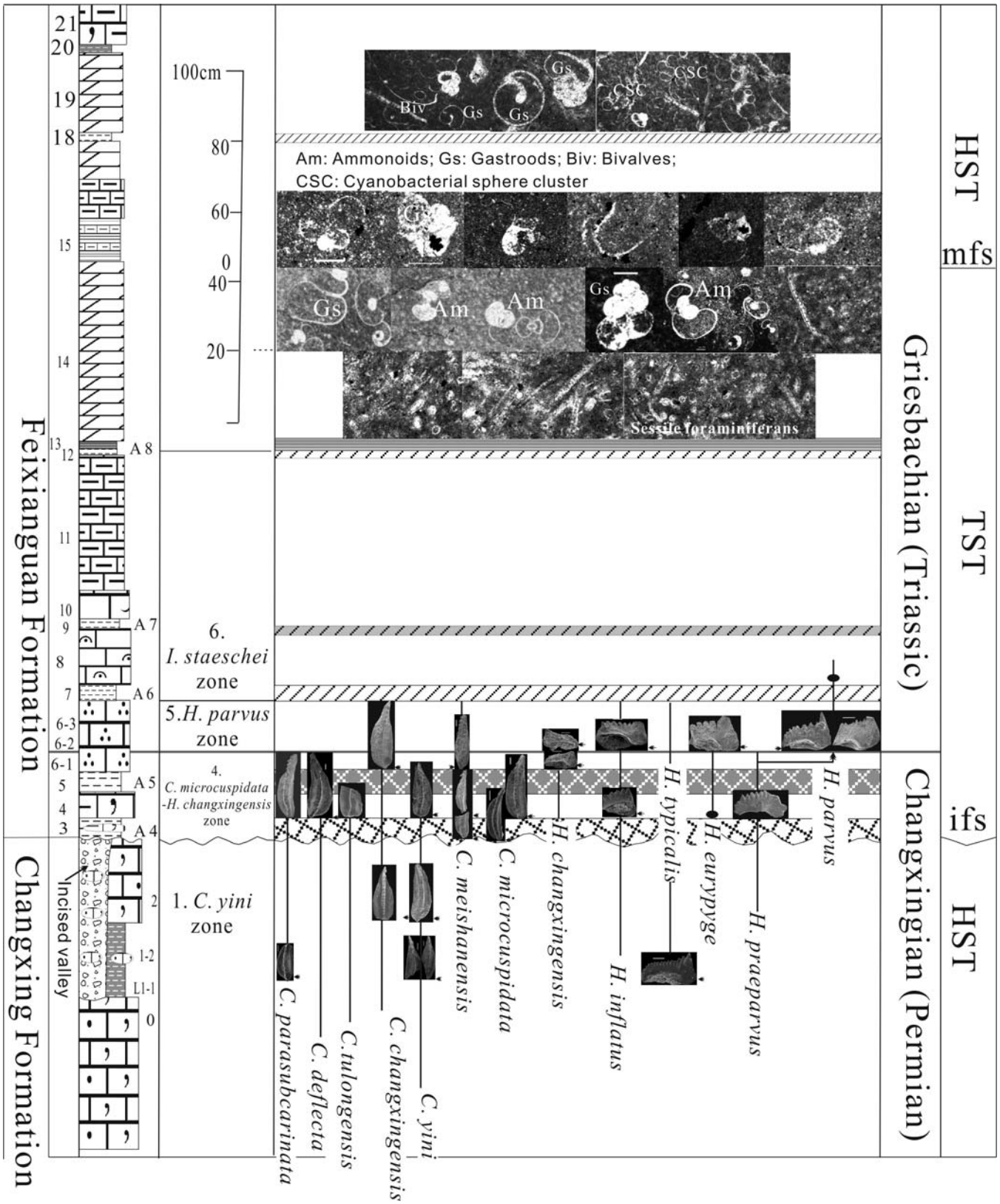

TEXT-FIGURE 5
Vertical distribution of conodont specimens through PTB in the Liangfengya section showing a columnar succession of the strata in platform interior in which ash bed 1, the *C. meishanensis* Zone with internal ash bed 2 , and the *C. taylorae* Zone with its basal ash bed 3 are absent due to subaerial unconformity.

16), *H. bicuspidate* (text-fig. 11. 18), *H. turgidus* (text-fig. 11. 19), *C. taylorae* (text-fig. 11.20) and *C. tulongensis* (text-fig. 11.23).

Occurrence: This conodont zone immediately overlies the maximum flooding surface in the Xiakou section (text-fig. 3). The maximum flooding surface can be distinguished by its dark color clay containing abundant Early Triassic fossils in South China.

Ash beds through the PTB and their relationship to conodont biozones

Eight ash beds were recognized as altered ash beds around the PTB in the Xiakou section (Hong et al. 2008; Shen et al. 2012). Except for abundant authigenic zircons and altered illite–montmorillonite, the ash beds do not contain terrigenous debris. Very thin ash beds with wide areal extent have been regarded as regional markers for stratigraphic comparison. If these ash beds can be assigned a stratigraphic level by comparison with related conodont zones, they would be an important marker for stratigraphic comparison in South China. This work attempts to detect and describe the stratigraphic significance of eight ash beds based on studies of the relationships between conodont zones and these ash beds (text-figs. 2, 3, 4, 7).

1) Ash bed 1 (A1) directly underlies the *C. meishanensis* conodont zone and consists of vitric tuffs from which no conodont specimens have been recovered. This ash bed is characterized by having varied thickness (0 to 30 cm thick). Thus, it is of lesser significance for stratigraphic comparison.

2) Ash bed 2 (A2) always appears as an internal ash bed of the *C. meishanensis* conodont zone in the basin-filling and some slope-filling sequences. It typically separates the *C. meishanensis* zone into two intervals; the lower interval yields moderate numbers of conodont specimens of *C. meishanensis* zone, whereas the upper interval contains fewer conodont specimens. In the shoreward direction (upper slope and platform interior), ash bed 2 is absent. This ash bed consistently comprises illite-montmorillonite minerals and authigenic zircons and never terrigenous debris. It is very thin (2-4 mm thick), but consistently present in basin-filling sequences and can be therefore regarded as a regional stratigraphic marker for identifying the *C. meishanensis* conodont zone and its regressive systems tract.

3) Ash bed 3 (A3) appears at the base of the *C. taylorae* conodont zone and lowstand system tract. It universally extends in the basin-filling sequences. In the strata of slope and platform interior, it is absent. This ash bed similarly contains illite-montmorillonite minerals and authigenic zircons but not terrigenous debris. It is also characterized by containing the first specimen of *C. taylorae* and other species and by having a consistent thickness (2.5-4mm). Therefore, it is regarded as regional marker that signifies the base of the *C. taylorae* conodont zone in South China (text-figs. 2, 7).

The spatial arrangements of ash beds 1, 2, and 3 appear as an offlapping framework (text-fig. 7) in which ash bed 1 occurs in platform, slope, and basin settings; and ash beds 2 and 3 are restricted to the toe-of-slope facies and basin settings. Clearly, this offlapping framework was a response to progradation of the shoreline and erosional leveling process during eustatic sea-level fall.

4) Ash bed 4 (A4) appears as at the base of the *H. changxingensis-C. microcuspidata* conodont zone and its initial sea-flooding section. It rests on a flattened surface and is widespread in the strata of platform interior, slope and basin (text-figs. 2 and 7). This ash bed comprises non-terrigenous illite-montmorillonite minerals and plenty of conodont speci-

TEXT-FIGURE 6

Photographs of specimens from the *C. yini* zone (figs. 1-14) and *C. meishanensis* zone (figs. 15-33) in Meishan-E (Msh), Xinmin (Xm), Zunyi (Zy), Liangfengya (Lfy), Huaying (Hy) and Xiakou (Xk) sections, scale bar= 100 mm.

1-6, 28 *Clarkina yini* Mei, Zhang and Wardlaw 1998, 1, oblique lateral view, Xm 3-1/001; 2, 3, oblique upper views, Zy1-2/ 004, 006; 4, oblique upper view, Hy 2/003; 5-6, oblique upper views, Hy4/007, 004; 28, upper view, Hy 11-2/004.

7-10, 25-27 *Clarkina changxingensis* (Wang and Wang 1981), 7, oblique upper view, Xm 3-3/003; 8, 9, oblique upper views, Hy 2/002, Hy 4/002; 10, upper view, Lfy 2/008; 25, upper view, Hy 11-2/006; 26, 27, upper views, Msh 24e /015, 025.

11 *Clarkina tulongensis* (Tian 1982), upper view, Hy 8/007.

12 *Claikina postwangi* (Tian 1993), oblique upper view, Hy 4/006.

13, 14 *Clarkina zhejiangensis* Mei 1996, 13, upper view, Js 110/4-016; 17, upper view, Hy 11-2/012.

15-23 *Clarkina meishanensis* Zhang, Lai and Ding 1995, 15, 16, upper views, Msh 24e-l/ 023, Msh 24e-u /003; 17, oblique upper view, Msh 24e-u/022; 18, upper view, Xk 251/005; 19, lateral view, Js 117/4-020; 20, oblique lateral view, Js 117/006; 21, 22, upper views, Xm 4-3/001, 003; 23, oblique upper view, Msh 24e-l/012; 24, upper view, Hy 11-3/001.

28 *Clarkina yini* Mei, Zhang and Wardlaw 1998, upper view, Msh 24e-l/028.

29 *Clarkina deflecta* (Wang and Wang 1981), upper view, Hy 11-2/002.

30 *Hindeodus eurypyge* Nicoll, Metcalfe and Wang 2002, Zy 2/006.

31 *Hindeodus latidentatus* Kozur, Mostler and Ranhimi-Yazd 1975, lateral view, Hy 11-2/011.

32 *Hindeodus typicalis* (Sweet 1970), lateral view, Hy11-2/012.

33 *Hindeodus praeparvus* Kozur 1996, lateral view, Hy 11-1/005.

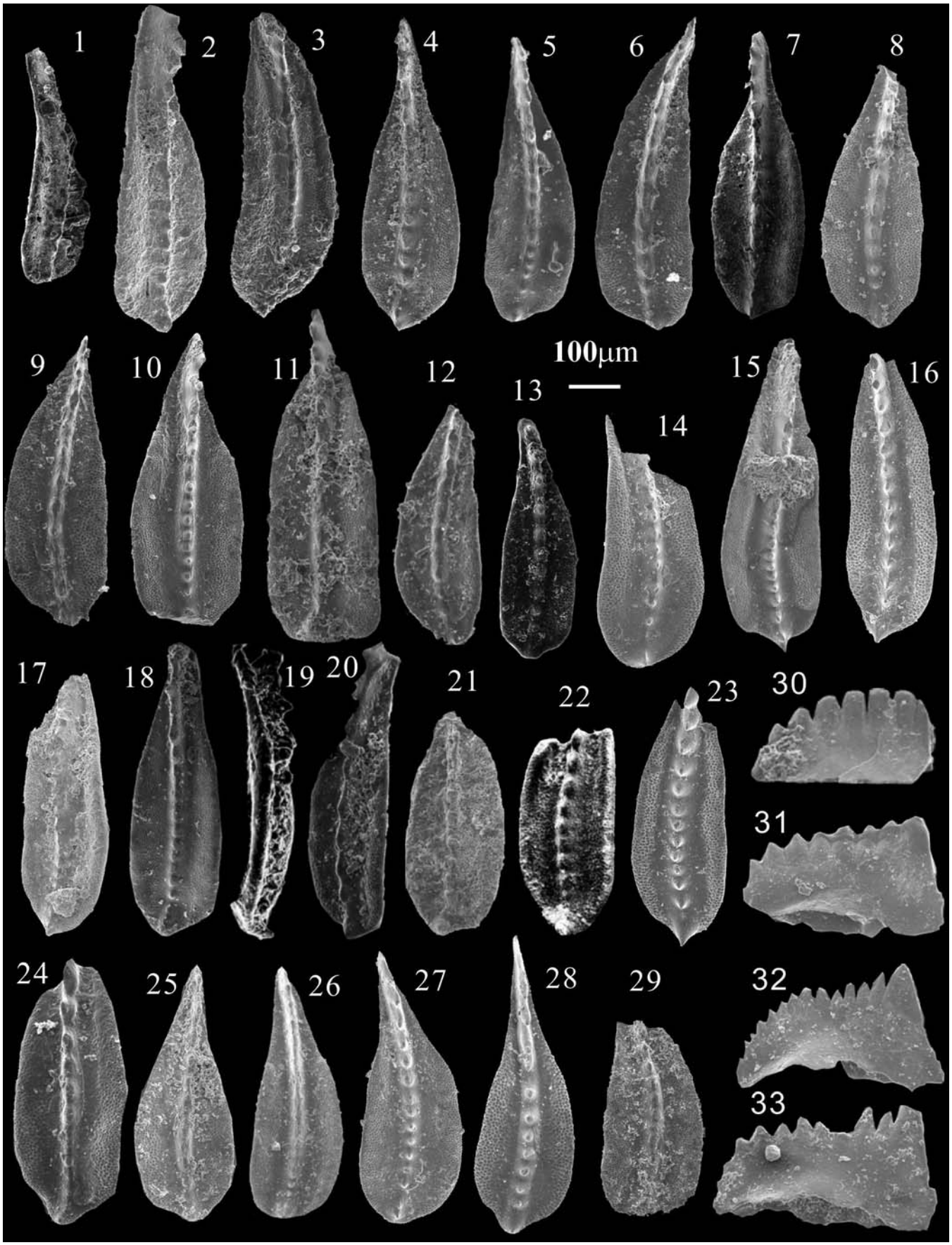
1
2
3
4
5
6
7
8
9
10
11
12
13
14
15
16
100μm
17
18
19
20
21
22
23
30
31
24
25
26
27
28
29
32
33

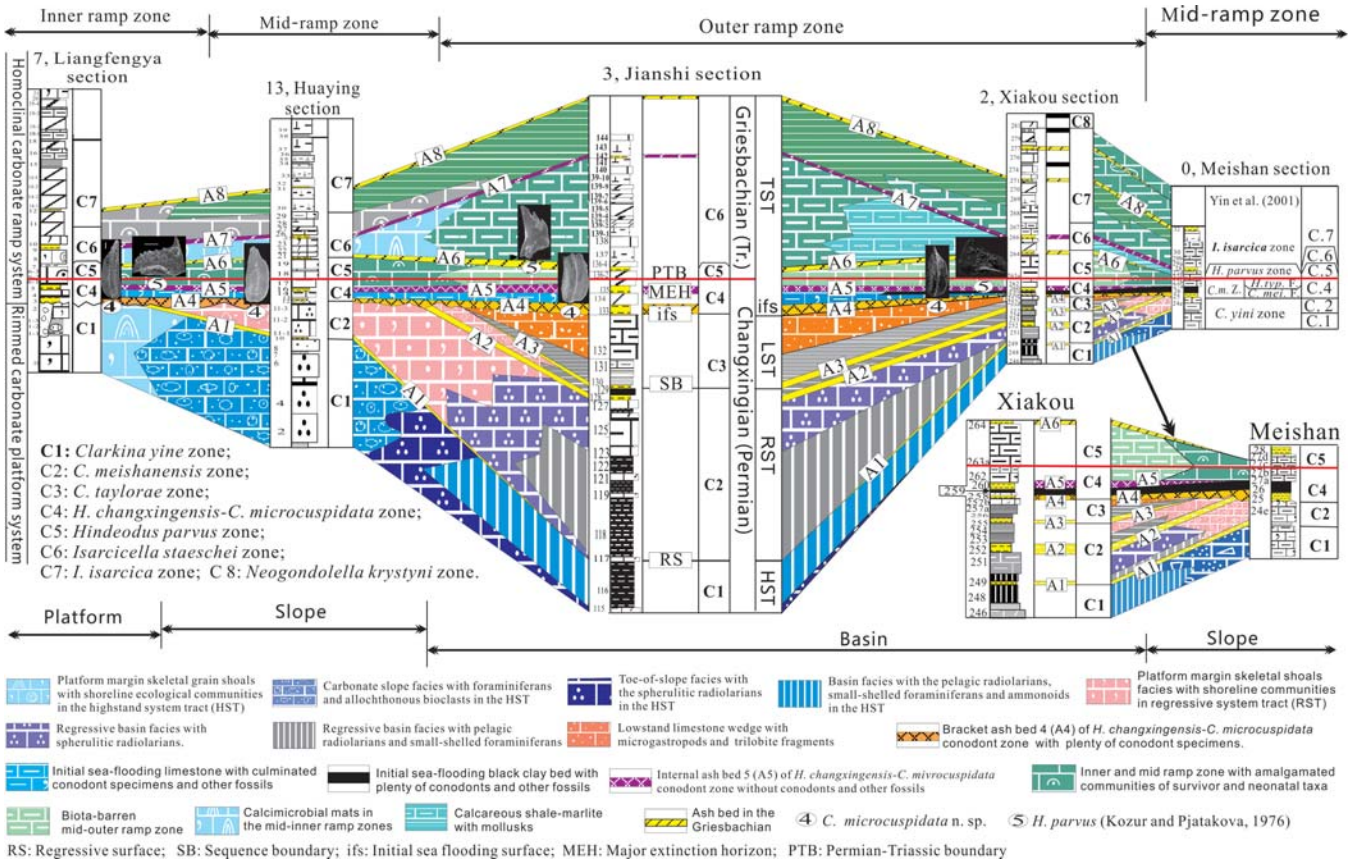

TEXT-FIGURE 7
Detailed cross-sections throughout Liangfengya, Huaying, Jianshi, Xiakou, and Meishan sections showing geographical variation of conodont zones, related ash beds, and facies: in the basin-filling sequences, there is a complete succession with eight conodont zones and eight related ash beds. In the slope-filling sequences, the *C. taylorae* Zone and its basal ash bed 3 is absent, whereas in the strata of the platform interior, ash bed 1, the *C. meishanensis* Zone and internal ash bed 2 are also absent.

mens of *C. microcuspidata*, *C. meishanensis*, *C. changxingensis*, *C. zhejiangensis*, and *H. praeparvus*. Therefore, it is recognized as a regional marker horizon for recognizing the base of the *H. changxingensis-C. microcuspidata* conodont zone and its initial sea-flooding section.

5) Ash bed 5 appears as an internal horizon of *H. changxingensis-C. microcuspidata* conodont zone. In addition to its widespread distribution and non-terrigenous, illite-montmorillonite compositon, this ash bed is barren of biotic components. Below this ash bed, the underlying section appears as fossiliferous limestone or black clay contains Changhsingian conodont populations (text-figs. 2 and 7) and abundant Permian fossils. Ash bed 5 should be considered a marker horizon for recognition of a major extinction event.

6) Ash bed 6 (A6) directly underlies the *I. staeschei* conodont zone. It simply consists of non-terrigenous illite-montmorillonite minerals and never terrigenous debris. The very thin ash should be considered as regional marker for identifying the lower limit of the *I. staeschei* conodont zone.

7) Ash bed 7 (A7) occurs within the *I. staeschei* conodont zone and comprises non-terrigenous illite-montmorillonite minerals in South China (text-figs. 2 and 7). It subdivides the *I. staeschei* conodont zone into two intervals in South China. More conodont specimens and Permian survival taxa occur in the lower interval, whereas there are few conodonts and no Permian survivors in the upper interval. Therefore, it should be regarded as regional marker for identifying final extinction horizon of survival taxa (text-fig. 2).

8) Ash bed 8 occurs within the *I. isarcica* conodont zone (text-figs. 2 and 7). In addition to comprising non-terrigenous illite-montmorillonite minerals, this ash bed also contains conodont specimens of *I. isarcica* and *H. parvus* (text-fig. 3). Below this ash bed, there are few conodont specimens except for the first appearance specimen of *I. isarcica*. In and above ash bed 8, there are many fossils of ammonoids, foraminifers, gastropods, and bivalves. In addition, the conodont genera *Hindeodus-Isarcicella-Ellisonia* can be observed (text-figs. 3 and 5). Therefore, this ash bed should be regarded as a regional marker at the midpoint of the *I. isarcica* conodont zone.

DISCUSSION

Different conodont successions through the PTB have been reported from the Meishan global stratotype section (Yin et al.

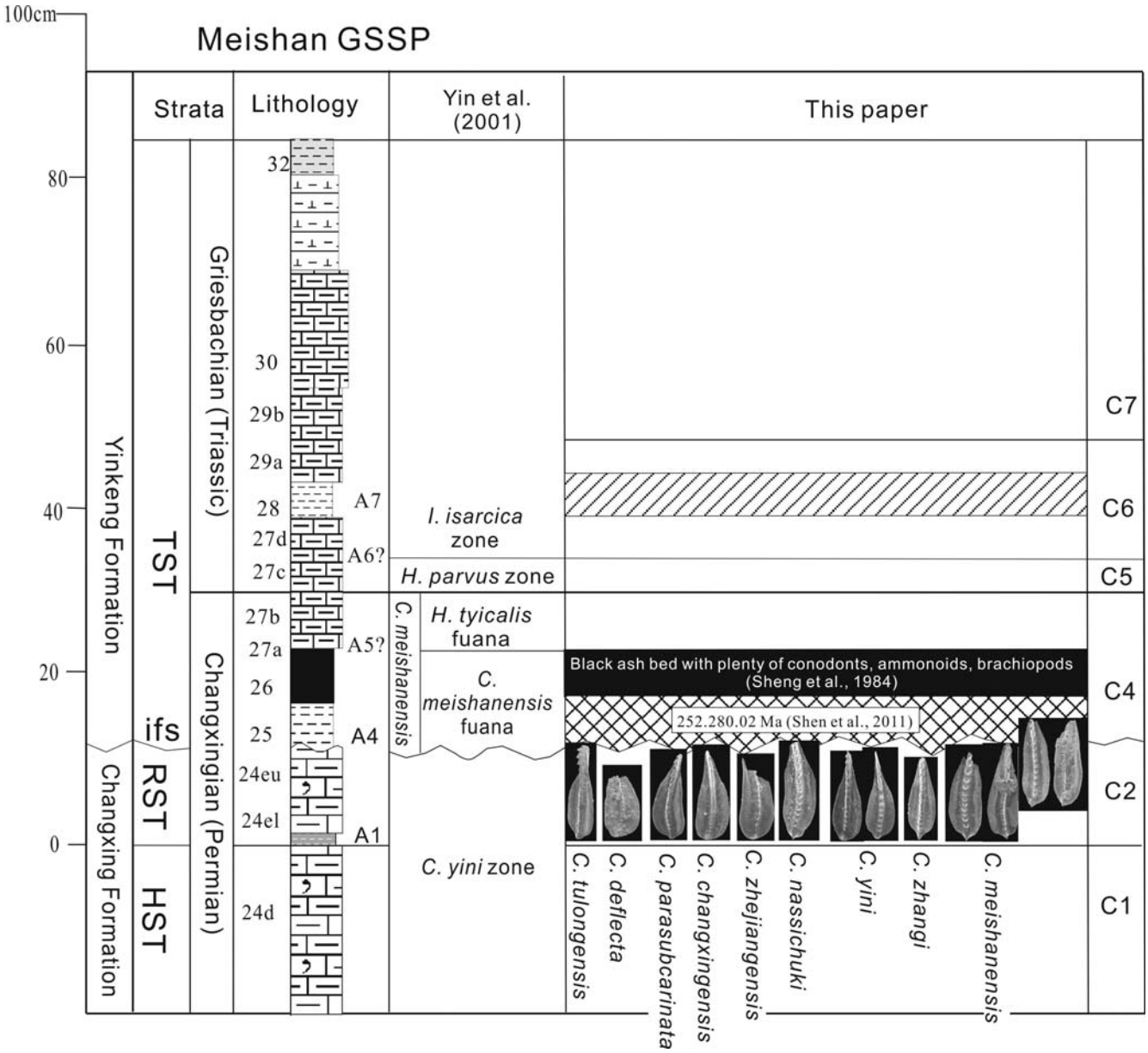

TEXT-FIGURE 8
Vertical distribution of conodont specimens through the PTB in the Meishan global stratotype section shows a columnar succession of slope-filing sequences in which the base of *C. meishanensis* conodont zone (C2) has extended down from the base of Bed 25 (Yin et al. 2001) to the base of Bed 24e, and the *C. taylorae* conodont zone (C3) with its basal ash bed 3 was absent due to subaerial unconformity.

2001; Zhang et al. 2007, 2009; Jiang et al. 2007). When the conodont succession from other sections (Ji et al. 2007; Chen 2008, 2009; Jiang et al. 2011) is considered, there is an even greater difference of conodont successions. Without a doubt, the global succession of conodont zones across the PTB should be consistent. Why is there such large difference at Meishan? Our studies of the conodont succession in condensed or incomplete columns may provide insight. Our comparison of the conodont stratigraphic ranges through the PTB among six sections in diverse paleogeographic settings resulted in a high-resolution conodont succession that was calibrated in the basin-filling sequences (text-figs. 3 and 4). It consists of the *C. yini* zone, *C. meishanensis* Zone, *C. taylorae* Zone, *H. changxingensis-C. microcuspdata* Zone, *H. parvus* Zone, *I. staeschei* Zone, *I. isarcica* Zone, and *N. krystyni* Zone, in ascending order. The applicability of the calibrated conodont succession not only has been verified by comparison of conodont stratigraphic ranges of the Xinmin, Jianshi, and Xiakou sections (text-fig. 2), but it can also be examined through comparison with other documented sections. Compared with conodont succession in the Chaotan section of Sichuan Province, South China (Fig. 2 of Ji, et al. 2007), the FA of *C. meishanensis meishanensis* exactly coincides with the lower limit of the *C. meishanensis* conodont zone in the Xinmin, Jianshi, and Xiakou sections, and the *C. taylorae-C. zhejiangensis -C. changxingensis yini* zone correlates to our *C. taylorae* zone. Moreover, compared with the

biostratigraphy around the PTB in Iran (Figs. 3-7 of Kozur 2007), the *C. hauschkei* zone + lower *C. meishanensis* conodont zone is equal to our *C. meishanensis* conodont zone because the *C. hauschkei* (Kozur 2004) can be recognized as a form of *C. meishanensis* (Zhang, Lai and Ding 1998). In addition, the upper *C. meishanensis* conodont zone of Iran could be correlated with the *C. taylorae* zone because a *C. taylorae* (Orchardi 1994) specimen was also recovered from the upper *C. meishanensis* zone in Iran (Kozur 2004). Consequently, the calibrated conodont succession in this work can be applied outside of South China.

Eight regional ash beds consistently occur around the PTB in South China (text-figs. 2 and 7), and these provide the opportunity to perform studies of the relationships between conodont zones and ash beds that contain important information (Shen et al. 2012). As reported in this work, ash beds 1 and 6 appear, respectively, at the upper limits of the *C. yini* and *H. parvus* zones; ash beds 3and 4 appear, respectively, at the lower limits of *C. taylorae* and *H. changxingensis*-*C. microcuspidata*, zones; and ash beds 2, 5, 7 and 8 occur, respectively, within the *C. meishanensis*, *H. changxingensis*-*C. microcuspidata*, *I. staeschei*, and *I. isarcica* zones. Moreover, ash beds 3, 4, and 8 contain recognizable conodont specimens. Therefore, every ash bed can be calibrated as a regional marker for identifying the correlative conodont zone and sequence stratigraphy in South China. Spatial arrangements of conodont zones and related ash beds in diverse geographic settings indicate three types of paleogeographic successions in South China (text-fig. 7). The complete succession of eight conodont zones and eight ash beds occurs in basin-filling sequences, such as the Xinmin, Jiashi, Xiakou, and Chaotian sections. In slope-filling sequences, such as in the Huaying and Zunyi sections, ash bed 3, the *C. taylorae* conodont zone, ash bed 2 and the upper part of the *C. meishanensis* conodont zone are absent. In the strata of the platform interior, such as the Liangfengya section, ash bed 1, all of the *C. meishanensis* conodont zone are also absent.

The global stratotype section at Meishan consists of a *C. yini* zone, a *C. meishanensis* zone, a *H. parvus* zone and an *I. isarcica* zone. The GSSP that was ratified by the IUGS in 2000 for the PTB was placed at the base of the *C. parvus* zone (Yin et al. 2001). Of the four biozones, the *C. meishanensis* zone was subdivided into *C. meishanensis* fauna in the lower part and *H. typicalis* fauna in the upper part (text-fig. 7). More detailed succession of conodont biozones in the Meishan section was established by Zhang et al. (2009) consisting of a *N. zhangi* -*N. yini* zone (Bed 24), *N. meishanensis* zone (Bed 25), *H. changxingensis* zone (Bed 26), *N. taylorae* zone (Beds 27a, and 27b), *H. parvus* zone (Bed 27c), *I. staeschei* zone (Bed 27d, Bed 28 and Bed 29a) and *I. isarcica* zone (Bed 29b), in ascending order. The works on Meishan section have demonstrated that the Triassic biostratigraphy is an international achievement, whereas the uppermost Permian biostratigraphy could not appear as a detailed succession because it was compressed. New work on conodont specimens from Bed 24e in the Meishan sec-

TEXT-FIGURE 9

Photographs of specimens from *C. taylorae* zone (figs. 1-10) and *H. changxingensis*-*C. microcuspidata* zone (figs. 11-38) in the Xiakou (Xk), Huaying (Hy), Liangfengya (Lfy), Zunyi (Zy), and Xinmin (Xm) sections, scale bar=100 mm,

1-4, 32, 33 *Clarkina taylorae* (Orchard 1994), 1, oblique upper views, Xm 5-1-2/161; 2, oblique upper view, Xm 10-5/ 001; 3, oblique upper view, Xk 255/013; 4, oblique upper view, Js 130-6/006; 32, oblique upper view, Xm 5-3-1/chen 006; 33, upper viw, Xk 260/2568.

5, 6, 21-24 *Clarkina meishanensis* Zhang, Lai and Ding 1995, 5, oblique upper view, Js 132/4-019; 6, oblique upper view, Xk 255/x-006; 21, oblique lateral view, Xm 5-1-2/085; 22, oblique upper view, Xm 5-1-2/051; 23, oblique lateral view, Xk 259b/003; 24, oblique lateral view, Xm 5-3-1/011. 7: *Clarkina nassichuki* (Orchard 1998), oblique upper view, Js 130-6/001.

8, 25 *Clarkina changxingensis* (Wang and Wang 1981), 12, upper views, Xk 257b/2163; 25, oblique upper view, Hy 14/004. 9: *Clarkina abadehensis* Kozur 2004, Xk 257b/z023.

10, 28, 29 *Clarkina parasubcarinata* Mei, Zhang and Wardlaw 1998, 10, oblique upper view, Xk 257 b/0012; .28, oblique upper view, Lfy 4-1/006; 29, oblique upper view, Xm 5-1-2/086.

11-19 *Clarkina microcuspidata* n. sp., 11, oblique upper view, Hy 13/010; 12, oblique lateral view, Lfy 3-2/004; 13, oblique upper views, Lfy 4-1/001; 14, oblique upper view, Xm 5-1-2/041; 15, 16, oblique lateral views, Xm 5-3-1/005, 001;17, oblique upper view, Xm 5-3-1/009; 18, oblique lateral view, Xk 259b/027; 19, oblique upper view, Xk 259b/004.

20 *Clarkina tulongensis* (Tian 1982), upper view, Xm 5-1-2/072.

26 *Hindeodus changxingensis* Wang 1995, lateral view, Xm 5-3-1/007.

27 *Clarkina yini* Mei, Zhang and Wardlaw 1998, oblique upper view, Js 136 /001.

30 *Clarkina zhejiangensis* Mei 1996, upper view, Xm 5-1-2/078.

31 *Clarkina orchardi* (Mei 1996), oblique upper views, Xm 5-1-2/081.

34, 35 *Hindeodus eurypyge* Nicoll, Metcalfe and Wang 2002. Lateral views, Zy 5/001; Xk 262 /2558.

36 *Hindeodus latidentadus* (Kozur, Mostler & Rahimi-Yazd 1975), Lateral view, Xk 262/1856.

37 *Hindeodus inflatus* Nicoll, Metcalfe and Wang 2002, lateral view, Xk 262/2579.

38 *Hindeodus praeparvus* Kozur 1996, lateral view, Xk 262/2523.

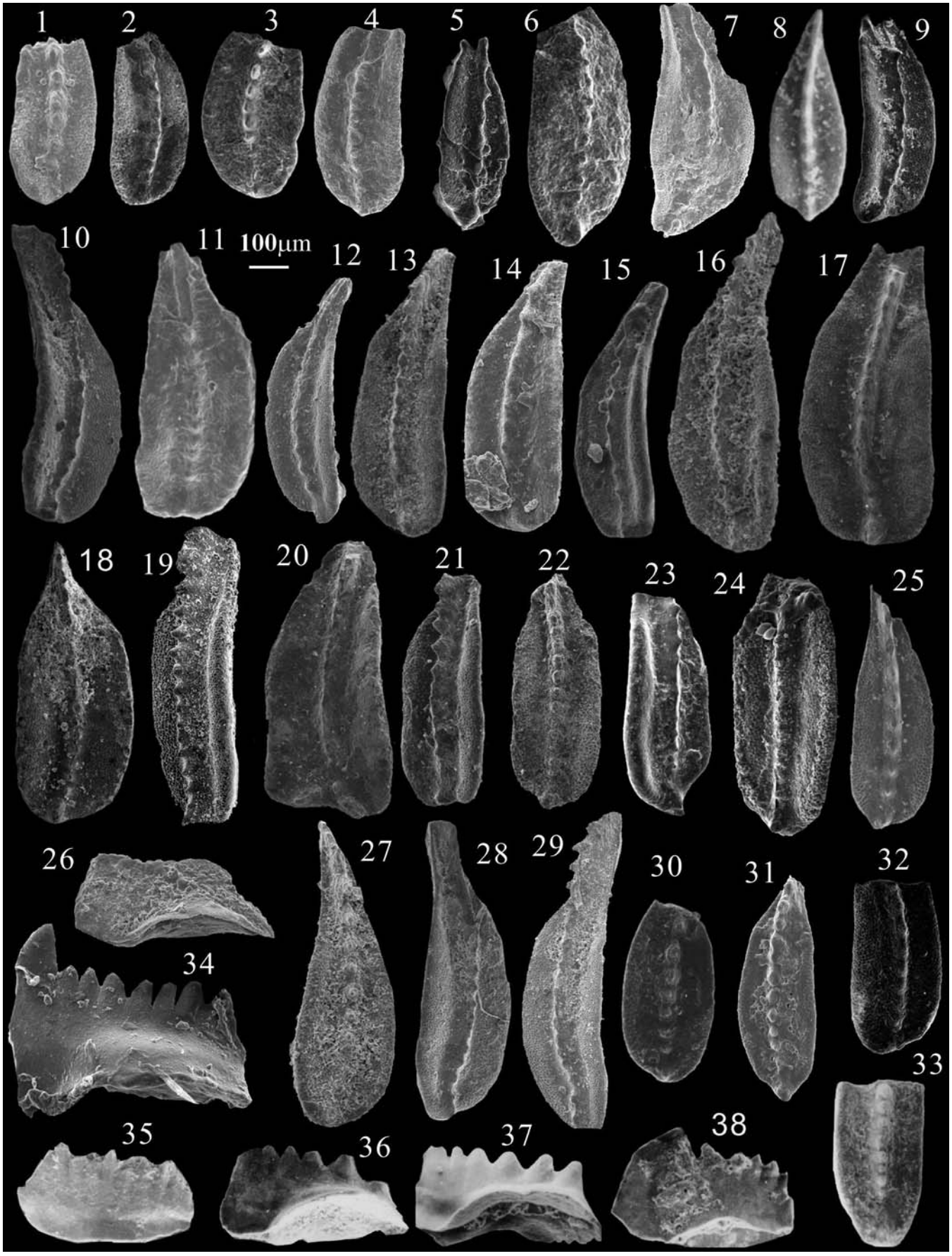
1
2
3
4
5
6
7
8
9
10
11
100μm
12
13
14
15
16
17
18
19
20
21
22
23
24
25
26
27
28
29
30
31
32
33
34
35
36
37
38

tion E (text-fig. 6.15-6.18; 6.23) has revealed that the lower limit of the *C. meishanensis* conodont zone should extend down from the base of Bed 25 to the base of Bed 24e (text-fig. 8). Furthermore, discovery of specimens of *H. changxingensis* from Bed 26 (Jiang et al. 2007; Metcalfe et al. 2009; Zhang et al. 2009) have proven that the *H. changxingensis-C. microcuspidata* conodont zone is present. In general, a complete succession of conodont zones should comprise the *C. yini* Zone, *C. meishanensis* Zone, *H. changxingensis-C. microcuspidata* Zone, *H. parvus* Zone, *I. staeschei* Zone, and *I. isarcica* Zone in ascending order in the Meishan section. Compared with calibrated conodont succession, ash bed 3 and the *C. taylorae* Zone appear to be absent by unconformity. Likewise, ash bed 2 and the upper part of the *C. meishanensis* Zone are also absent by unconformity. Therefore, the Meishan section would have been formed in the slope settings (text-fig. 7), in which the unconformity occurs at the base of Bed 25, which correlates to ash bed 4 of the calibrated succession. Clearly, the zircon U/Pb age 252. 28±0.03 Ma (Shen et al. 2011) from Bed 25 indicates the time of the initial sea-flooding event. The age of the end-Permian extinction might be later.

CONCLUSIONS

1) A high-resolution succession of conodont zones through the Permian-Triassic boundary was calibrated based on comparison of conodont stratigraphic ranges in six section from diverse paleogeographic settings in South China, including the *C. yini* , *C. meishanensis*, *C. taylorae*, *H. changxingensis-C. microcuspidata*, *H. parvus*, *I. staeschei I. isarcica*, and *N. krystyni* Zones. Comparison with the documented Chaotian section and the sections in Iran demonstrated that the calibrated conodont succession has significance beyond South China.

2) Eight regional ash beds around the PTB have been calibrated as regional markers for recognizing conodont zones and making stratigraphic comparisons between the conodont zones and ash beds in South China.

3) The spatial arrangements of the conodont zones and related ash beds present three types of paleogeographic successions of conodont zones. Contiguous, continuous conodont successions with eight conodont zones and related eight ash beds occur in the basin-filling sequences. In slope-filling sequences, the ash bed 3 and the *C. taylorae* conodont zone are missing by subaerial unconformity, and in the strata of platform interior, the ash bed 1 and all of the *C. meishanensis* zone with internal ash bed 2 are also absent.

TAXONOMY

In addition to the index species *H. parvus* that was detailed in Kozur and Pjatakova (1976), Nicoll, Metcalfe and Wang (2002), Ji et al. (2007), Chen et al. (2008) and *H. changxingensis* that was described by Wang (1995) and Metcalfe et al. (2007), other pivotal species for distinguishing conodont zones in calibrated succession are described below.

Phylum CHORDATA Bateson 1886
Class CONODONTIA Eichenberg 1930
Subclass CONODONTI Branson 1938
Order PRIONIODINIDA Sweet 1988
Family GONDOLELLIDE Lindstrom 1970
Genus *Clarkina* Kozur 1989

Type species: *Clarkina leves* Kozur, Mostley and Pjatakova 1976

Clarkina meishanensis Zhang, Lai and Ding 1995
Text-figures 6.15–6.24; text-figures 9.5–9.6, 9.21–9.24.

Clarkina sp. nov. WANG 1995, pl. 1, figs. 2-4.
Clarkina meishanensis n. sp. – ZHANG, LAI AND DING 1995, p. 674, pl. 2, figs. 4-6. – ZHANG et al. 1996 in YIN et al., p. 62, pl. 7, figs. 5, 12, 13. – ORCHARD AND KRYSTYN 1998, p. 358-360, pl. 1, figs. 10-14, 17-19, 26-28. – KOZUR 2004, p. 46, pl. 2, figs 13, 15, 23-25.
Neogondolalla meishanensis (Zhang, Lai and Ding), ORCHARD and KRYSTYN 1998, p. 358-360, pl. 1, figs. 10-14, 17-19, 26-28.

TEXT-FIGURE 10
Photographs of conodont specimens from *H. parvus* zone (figs. 1-11, 20) and *I. staeschei* zone (figs. 12-19, 21-24) in the Xinmin (Xm), Zunyi (Zy), Liangfengya (Lfy), Jianshi (Js) and Xiakou (Xk) sections, scale bar=100 mm.

1a, b, 2–6, 14, 17, 18 *Hindeodus parvus* (Kozur and Pjatakova 1976), 1a, outer lateral view, Xk 263a/1116-2-5a; 1b, upper view, Xk263a 1116-2-5b; 2, 3, inner lateral views, Lfy 6-2/003, 002; 4-6, lateral view, Xm 5-3-3/001, 002, 006; 14a, lateral view, Xk 265c/1116-3-1a; 14b, upper view, Xk265c/1116-3-1b; 17, 18, lateral view, Xk 267-1/z001, Xk 267-1/2565.

7a, b *Hindeodus latidentatus* (Kozur, Mostler & Rahimi-Yazd 1975), 7a, lateral view, Xk 263a /1116-2-3a, 7b; upper view, Xk 263a/1116-2-3b.

8a, b, 20 *Hindeodus inflatus* Nicoll, Metcalfe and Wang 2002. 8a, lateral view, Xk263a /1116-2-15a; 8b, upper view, Xk263b/1116-2-15b; 20, lateral view, Lfy 6-2/009.

9a, b; 15a, b *Hindeodus preaparvus* Kozur 1996, 9a, lateral view, Xk 263a /1116-2-10a; 9b, upper view, Xk 263a/1116-2-10b; 15a, lateral view, Xk 265c /1116-3-2a; 15b, upper view, Xk 265c/1116-3-2b.

10a, b, 16a, b, 19 *Hindeodus eurypyge* Nicoll, Metcalfe and Wang 2002; 10a, lateral view, Xk 263a /1116-2-14a; 10b, upper view, Xk 263a/1116-2-14b; 16a, lateral view, Xk 265a /1116-6-1a; 16b, upper view, Xk265a/ 1116-6-1b; 19, lateral view, Xk 267-2/z004.

11 *Hindeodus changxingensis* Wang c-y 1995, oblique lateral view, Lfy 6-2/007.

12, 13 *Isarcicella staeschei* Dai and Zhang 1989.12, lateral view, Xk265-b/x006; 13, upper view, Xk265a/2885.

21, 24 *Clarkina orchard*, Mei 1996, 21, oblique upper view, Zy14/003; 24, upper view, Xm 5-5-1/001.

22 *Clarkina zhejiangensis* Mei 1996, Zy14/001.

23 *Clarkina microcuspidata* n. sp., oblique upper view, Zy 14/002.

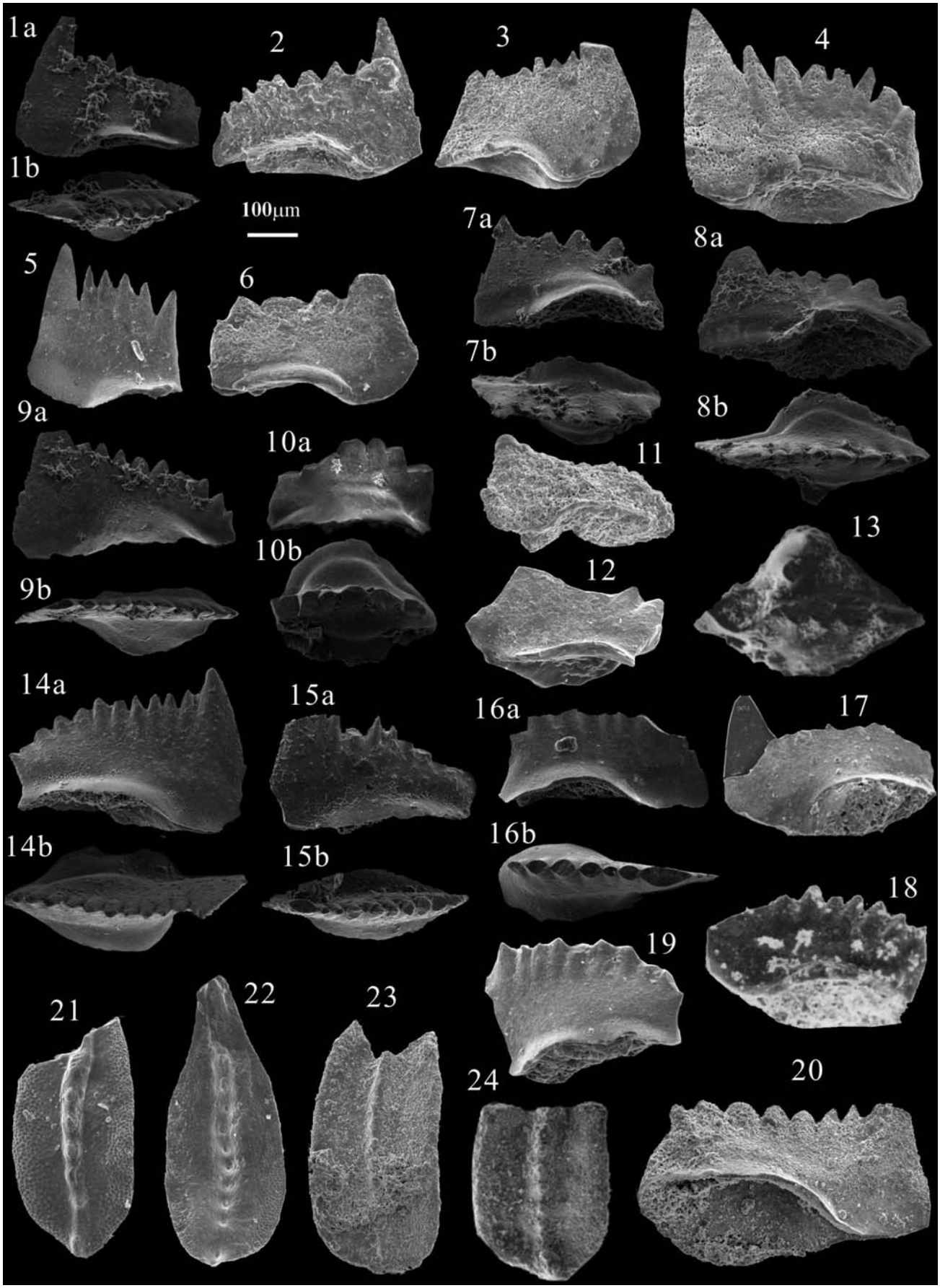
1a
2
3
4
1b
100μm
7a
8a
5
6
7b
9a
10a
11
8b
13
10b
12
9b
14a
15a
16a
17
14b
15b
16b
18
19
21
22
23
24
20

Clarkina meishanensis meishanensis Zhang, Lai and Ding. – MEI, ZHANG and WARDLAW 1998, pl. V, figs. R, H, K, P. – XIA et al. 2004, pl. 1, figs. 2, 3. – WANG and XIA 2004, p. 37, figs. 2.1-.3. – JI et al 2007, p. 50, Fig. 3.3-3.5, 3.12-3.14. – CHEN et al. 2008, p. 103, pl. 1, figs 9-14.
Clarkina hauschkei KOZUR 2007, pl. 1, fig. 27.

Diagnosis: The Pa element has a broadly subrectangular platform with narrowly rounded or pointed posterior termination and approximately parallel lateral sides, an anterior platform which is abruptly lower and narrow at posterior fourth, and the denticles on the carina are gradually decreasing posteriorly in height and size. There is a large high, and erect or slightly inclined cusp that is terminally located and separated from nearby denticles, with adcarina furrows deep and narrow.

Remarks: This species differs from the ancestor in having a broad subrectangular platform with parallel lateral margins in the middle portion, an abruptly lower and narrow anterior platform, and discrete denticles, whereas *C. zhangi* has a drop-like platform with a straight and tapering anterior portion.

Occurrence: The lowermost specimens are newly recovered from Bed 24e, which extends down at the base of a low-standing systems tract (Yin et al. 2001) in the Meishan section (text-fig. 8). In the Xiakou, Jianshi, Huaying, and Xinmin sections in South China and several sections in Iran (Kozur 2007), the lowermost specimens also extend down far away from the PTB (text-fig 6.18-6.22, 6.24). In the Liangfengya section, the *C. meishanensis* Zone is absent, and only evolved specimens appear above the unconformity (text-figs. 2 and 3).

Clarkina microcuspdata Zhang, Xia, Feng, Gao, Zhong and Wu, **n. sp.**
Text-figures 9.11–9.19; text-fig. 10.23

Neogondolella taylorae Orchard, JIANG et al. 2007, pl. II, fig. 32 (only).
Neogondolella deflecta (Wang and Wang), JIANG et al. 2007, pl. II, fig. 18 (only)
Clarkina deflecta (Wang and Wang), WANG C-Y 1995, pl. I, fig. 8 (only).
Clarkina aff. *deflecta* (Wang and Wang), MEI ET AL. 1998, pl. V. Fig B (only).

Materials: More than fifteen specimens with distinctive morphology were recovered from the samples Xm5-1-2, 5-3-1, and 5-3-2 in Xinmin section (text-fig. 4), from the samples Lfy 3 and 4 in Liangfengya section (text-fig. 5), from the samples Js 134 and 138 in Jianshi section (texi-fig. 2), from the sample Hy 13 in Huaying section (text-fig. 2), and from the sample Xk 259a in Xiakou section (text-fig. 3).

Diagnosis: A species of *Clarkina* in which the Pa element of the juvenile and adult specimens has a slightly broad platform that is widest at the midpoint, with a bluntly rounded and deflected posterior end, a lower carina bearing appressed and small nodes, an atrophied cusp abutting an accessory node nearby and forming a small double cusp, an outstanding gap containing two smaller nodes between the cusp and posteriormost node, and deep but smooth adcarina furrows.

Description: The Pa element has a slightly broad platform that is widest at the midpoint, with a blunt to rarely rounded, and asymmetrical posterior end, a lower and abruptly narrowing anterior part with four higher anterior denticles, a lower mid-posterior carina bearing 11–13 small and appressed nodes, an atrophied and terminally located cusp closely abutting to and partially merging with an accessory node nearby and forming a "couple cusp", an outstanding gap between the "couple cusp" and the carina. The whole carina is lower and slightly curving, with a deflected posterior tip. The platform margins are upturned, forming deep and long-extended adcarina furrows.

Comparison: This new species differs from other coexistent species in having a distinctive morphology. It resembles *C. parasubcarinata* in having a slightly broad platform and asymmetric posterior platform end but differs greatly from it in having a lower carina bearing small appressed nodes, an atrophied micro-cusp with an accessory node nearby, and a gap between the cusp and carina. It also differs from *C. meishanensis* (Zhang, Lai, and Ding) in having a slightly broad platform with a bluntly

TEXT-FIGURE 11
Photographs of conodont specimens from *I. isarcica* zone (figs. 1-11; 17) and *N. skystyni* zone (figs.12-16, 18-23) in the Xiakou (Xk) section, scale bar=100 mm.

1 *Isarcicella isarcica* Huckriede 1958, upper view, Xk268/ 1846.

2a, b *Isarcicella staeschei* (Dai and Zhang 1989), 2a, upper view, Xk271/2883; 2b, lateral view, Xk 271/2559.

3-6, 12-16 *Hindeodus parvus* (Kozur and Pjatakova,1976), 3-5, lateral views, Xk274/2543, 2151, 2563; 6, lateral view, Xk276/2521; 12-14, lateral view, Xk 281/x015, 1855, Xk282-1/2887; 15-16, lateral view, Xk281/x011, x010.

7 *Hindeodus typicalis* (Sweet 1971), lateral view, Xk276/1851.

8-9 *Hindeodus eurypyge* Nicoll, Metcalfe and Wang, 8, lateral view, Xk274/1844; 9, lateral view, X 276/2154.

10: *Hindeodus praeparvus* Kozur 1996, lateral view, Xk276/1861. 11: *Hindeodus changxingensis* Wang 1995, literal view, Xk276/1852.

17-18 *Hindeodus bicuspidate* Kozur 2004, 17, lateral view, Xk276/1850; 18, lateral view, Xk281/2881.

19 *Hindeodus turgidus* (Kuzor, Mostler and Rahimi-Yazd 1975), lateral view, Xk281/2884.

20 *Clarkina taylorae* Orchard 1994, upper view, Xk283-1/2888.

21, 22 *Clarkina krystyni* Orchard 1998, 21 oblique lataral view, 281/2889; 22, lateral view, Xk283-1/2890.

23 *Clarkina tulongensis* (Tian 1982), Oblique upper view, Xk283-1/2891.

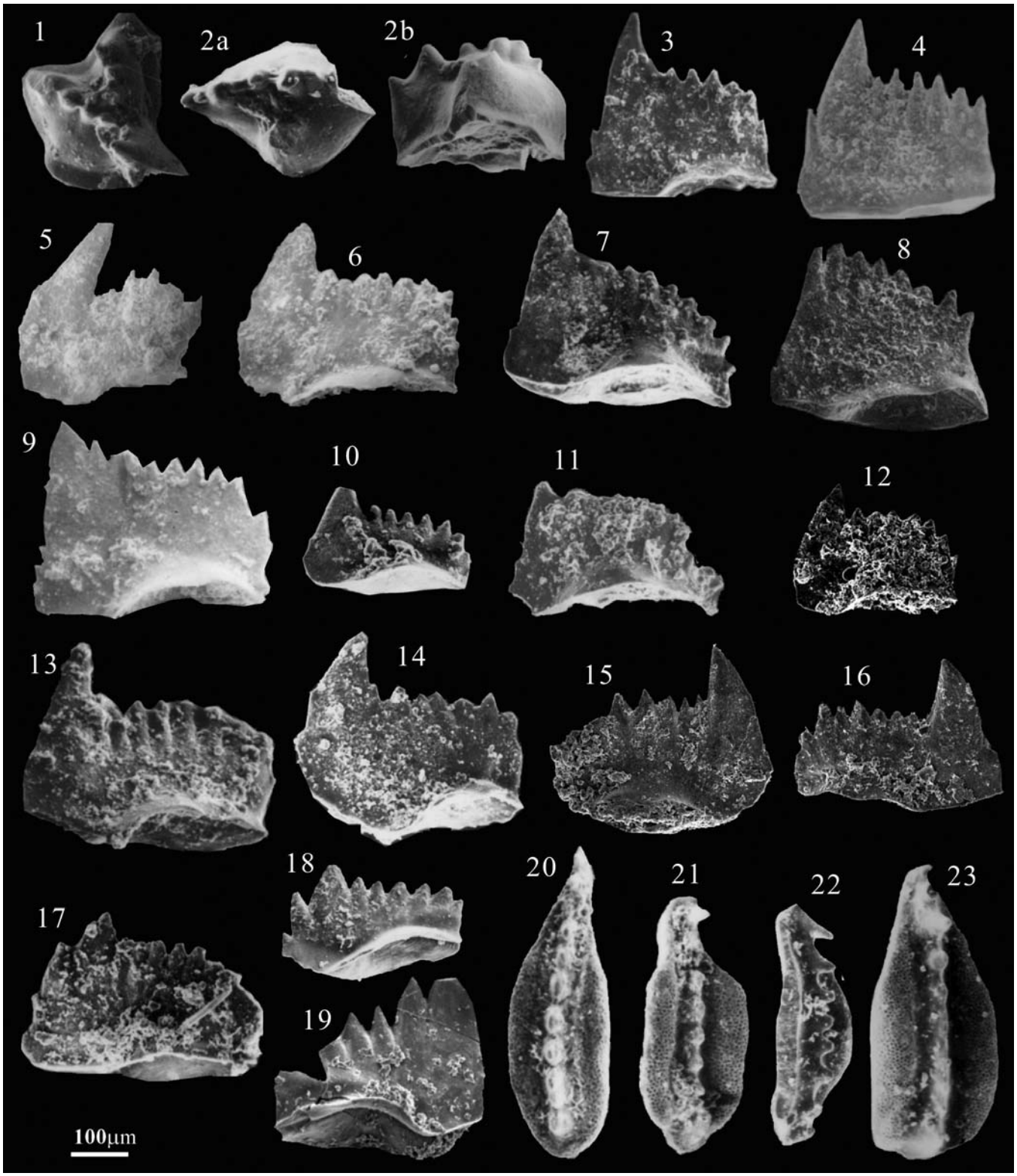
1
2a
2b
3
4
5
6
7
8
9
10
11
12
13
14
15
16
17
18
19
20
21
22
23
100μm

TABLE 1
Conodont correlation through PTB between GSSP and Xiakou sections.

<table>
<tr><th rowspan="2">Stage</th><th rowspan="2">Sequence</th><th colspan="2">Xiakou section (This paper)</th><th colspan="3">Meishan global stratotype section</th></tr>
<tr><th>No. of Beds</th><th>Conodont biozones</th><th>No. of Beds</th><th colspan="2">Yin et al. (2001)</th><th>Zhang et al. (2009)</th></tr>
<tr><td rowspan="15">Griesbachian (Triassic)</td><td>HST</td><td>Bed 281</td><td>N. krystyni Zone</td><td></td><td rowspan="15" colspan="2"></td><td rowspan="6">I. isarcica Zone</td></tr>
<tr><td>mfs.</td><td>Bed 178-280</td><td rowspan="6">I. isarcica Zone</td><td></td></tr>
<tr><td rowspan="13">TST ifs.</td><td>Bed 277</td><td></td></tr>
<tr><td>Bed 272-276</td><td></td></tr>
<tr><td>Bed 271 (A 7)</td><td></td></tr>
<tr><td>Bed 268-270</td><td>Bed 29b</td></tr>
<tr><td>Bed 267</td><td rowspan="3">I. staeschei Zone</td><td>Bed 29a</td><td rowspan="4">I. isarcica Zone</td></tr>
<tr><td>Bed 266 (A 6)</td><td>Bed 28</td></tr>
<tr><td>Bed 265</td><td>Bed 27d</td></tr>
<tr><td>Bed 264 (A 5)</td><td rowspan="2">H. parvus Zone</td><td>Absent</td><td colspan="2" rowspan="2">H. parvus Zone</td><td rowspan="2">H. parvus Zone</td></tr>
<tr><td>Bed 263</td><td>Bed 27c</td></tr>
<tr><td rowspan="10">Changhsingian (Permian)</td><td>Bed 262</td><td rowspan="5">H. changxingensis -C. microcuspidata Zone</td><td>Bed 27b</td><td rowspan="9">C. meishanensis zone</td><td>H. typicalis fauna</td><td rowspan="2">N. taylorae Zone?</td></tr>
<tr><td>Bed 261</td><td>Bed 27a</td></tr>
<tr><td>Bed 260 (A 4u)</td><td rowspan="3">Bed 26</td><td rowspan="8">C. meishanensis fauna</td><td rowspan="3">H. changxingensi Zone</td></tr>
<tr><td>Bed 259</td></tr>
<tr><td>Bed258 (A 4l)</td></tr>
<tr><td>Bed 257</td><td rowspan="3">C. taylorae Zone</td><td rowspan="3">Absent</td><td rowspan="3">Absent</td></tr>
<tr><td>Bed256</td></tr>
<tr><td>Bed 255 (A 3)</td></tr>
<tr><td rowspan="4">LST</td><td>Bed 253-254</td><td rowspan="4">C. meishanensis Zone</td><td rowspan="4">Bed 25</td><td rowspan="4">N. meishanensis Zone</td></tr>
<tr><td>Bed 252 (A 2)</td></tr>
<tr><td>Bed 250, 251</td></tr>
<tr><td>Bed 249 (A 1)</td></tr>
<tr><td>HST</td><td>Bed 248</td><td>C. zhangi-C. yini</td><td>Bed 24</td><td colspan="2">-C. yini Zone</td><td>N. zhangi-N. yini</td></tr>
</table>

rounded and asymmetrical posterior end, a micro (atrophied) cusp with an accessory node nearby, and a lower carina bearing appressed nodes.

Etymology: The nomenclature of *C. microcuspidata* is based on its distinctive morphology, including an atrophied micro-cusp.

Holotype: The specimen in text-fig. 9.13 that repository in the State Key Laboratory of Biogeology and Environmental Geology, China University of Geosciences, Wuhan, 430074, China.

Occurrence: This new species was derived from *C. meishanensis* at the uppermost Changhsingian Stage. Its lowermost specimens always occur in ash bed 4 or overlying limestone intercalations in the Xinmin, Zunyi, Liangfengya, Huaying, Jiashi, Xiakou, Huazhishan, and Meishan sections. Consequently, it is regarded as an index fossil for defining a new *H. changxingensis - C. microcuspidata* conodont zone. Upward, it persists through the PTB and into the lower Griesbachian.

Clarkina taylorae (Orchard et al. 1994)
Text-figures 9.1–9.4, 9. 32-9. 33; text-figure11.20

Gondolella orientalis (Barskov and Korolava) BHATT 1981b, p. 202, pl.1, figs. 7,8, 15, 16, 29, 30; pl. 2, figs. 1-3, 12-13, 18, 19.
Neogondolella taylorae ORCHARD et al. 1994, p. 833, pl. 2, figs. 9-12, 15, 16, pl. 3, fig. 15. – ORCHARD and SKTSTYN 1998, p. 360-362, pl. 2, fig. 1-9, 13-22. – JIANG et al. 2007, pl. II, figs. 29-34; pl. III, figs. 1-7, 28.
Clarkina taylorae Orchaid, MEI 1996, p. 145, pl. 18.2, fig. 15. JI et al. 2007, p. 52, Fig. 4. 24.

Diagnosis: The Pa element has an elongate oval platform, broadest medially or with subparallel lateral margins, and a rounded or bluntly rounded posterior end. The blade-carinal denticles are generally low and moderately discrete and pass in a prominent upright cusp surrounded by a visible posterior brim.

Remarks: The species of brim-bearing *Clarkina* include *C. xiangxingensis* (Tian), *C. carinata* (Clark), and *C. taylorae* (Orchard) in the upper Changhsingian. Of these, *C. xiangxingensis* has an elongate platform and fused carina; *C. carinata* differs from the others in having a button at the posterior platform end, whereas *C. taylorae* is characterized by discrete denticles and a round posterior end with a visible brim.

Occurrence: The lowermost specimen was recovered from the maximum regressive systems tract in the basin zone. In slope and platform zones, there is an absence of the FA of *C. taylorae*. Therefore, the species is regarded as an index fossil for defining the *C. taylorae* zone.

ACKNOWLEDGMENTS

This research was supported by the Natural Science Foundation of China (Grant Nos. 41372039 and 40572068). We thank Prof. Zhang S.X. for taking the SEM images of conodont specimens in the State Key Laboratory of Geological Processes and Mineral Resources and Prof. Zhang Kexin of Faculty of Earth Science, China University of Geosciences, for helping with identification of conodont specimens and providing useful suggestion. We are especially thankful to Prof. I. Metcalfe, Asia Centre University of New England, Australia for the thoughtful review of our manuscript and providing of very useful suggestions. Thanks to Lucy Edwards, Editor of *Stratigraphy*, for help with our text and figures.

REFERENCES

BATESON, W., 1886. The ancestry of the Chordata. *Quarterly Journal of Microscopical Science,* 26: 218–571.

BHATT, D. K., JOSHI, V. K. and ARORA, R. K., 1981b. Morphological observations on conodonts from Otoceras bed of Himalaya. In: Badve, R. M., Borkar, V. D., Ghare M. A. and Rajshekhar, C., Eds., *Proceedings of the X Indian Coloquium on Micropaleontology and Stratigrapy*, 197–210. Pune: Maharashtra Association for the Cultivation of Science.

BOWRING, S. A., ERWIN, D. H., JIN, Y., MARTIN, M. W., DAVIDEK, K. and WANG, W, 1998. U/Pb zircon geochronology and tempo of the end-Permian mass extinction. *Science*, 280: 1039–1045.

BRANSON E. B., 1938. *Stratigraphy and paleontology of the Lower Mississippian of Missouri. Part I.* Columbia: University of Missouri. Studies, no. 13 (3), 208 pp.

CHEN, J., BEATTY, T. W., HENDERSON, C. M. and ROWE, H., 2009. Conodont biostratigraphy across the Permian–Triassic boundary at the Dawen section, Great Bank of Guizhou Provice, South China: Implications for the late Permian extinction correlation with Meishan. *Journal of Asian Earth Sciences*, 36: 442–458.

CHEN, J., HENDERSON, C. M., and SHEN, S. Z., 2008. Conodont succession around the Permian-Triassic boundary at the Huangzhishan section, Zhejiang and its stratigraphic correlation. *Acta Paleontologica Sinica*, 47: 91–114.

CHEN, Z. Q. and BENTON, M. J., 2012. The timing and pattern of biotic recovery following the end-Permian mass extinction. *Nature Geoscience*, 5: 375–383.

CLARK, D. L., 1959. Conodonts from the Triassic of Nevada and Utah. *Journal of Paleontology*, 33: 305–312.

DAI, J. and ZHANG, J., 1989. [Conodonts]. In: Li, Z., Zhang, L., Dai, J., Jin, R., Zhu, X. Zhang, J. and Li, H., Eds., [*Study on the Permian-Triassic biostratigraphy and event stratigraphy of northern Sichuan and southern Shanxi*], 38–45. Beijing: Ministry of Geology and Mineral Resuources, Geological Memoirs, Series 2, no. 9 (in Chinese).

EICHENBERG, W., 1930. Conodonten aus dem Culm des Harzes. *Palaontilogische Zeitschrift*, 12: 177–182.

ELLISON, S., 1941. Revision of the Pennsylvanian conodonts. *Journal of Paleontology*, 15: 107–143.

HONG, H. L., ZHANG N., LI, Z., XUE, H. J., XIA, W. C. and YU, M., 2008 Clay mineralogy across P-T boundary of Xiakou section, China: Evidence of clay provenance and environment. *Clays and Clay Minerals*, 56: 131–143.

HUCKRIEDE, R., 1958. Die conodonten der mediterranen Trias und ihr stratigraphischer Wert. *Palaontologische Zeistchrift*, 32: 1–141.

JI, Z., YAO, J., ISAZAKI, Y., MATSUDA, N. and WU G., 2007. Conodont biostratigraphy across the Permian-Triassic boundary at Chaotian, in northern Sichuan, China. *Palaeogeography, Palaeoclimatology, Palaeoecology*, 252: 39–55.

JIANG H., LAI X., LUO G., ALDRIDGE, R., ZHANG K. and WIGNALL, P., 2007. Restudy of conodont zonation and evolution across the P/T boundary at Meishan section, Changxing, Zhejiang, China. *Global and Planetary Change,* 55: 39–55.

JIN, Y. G., WANG, Y. J., WANG, W., SHANG, Q. H., CAO, C. Q. and ERWIN, D. H., 2000. Pattern of marine mass extinction near the Permian–Triassic boundary in South China. *Science*, 289: 432–436.

KOZUR, H. W., 1989. The taxonomy of the Gondolellid conodonts in the Permian and Triassic . *Courier Forschungsinstitut Senckenberg.* 117, 409–469.

———, 1996. The conodonts *Hindeodus, Isarcicella* and *Sweetohindeodus* in the uppermost Permian and lowermost Triassic. *Geologia Croatica*, 49: 81–115.

———, 2004. Pelagic uppermost Permian and Permian-Triassic boundary conodonts of Iran. Part 1: Taxonomie. *Hallesches Jahrbuch für Geowissenschaften, Beiheft*, 18: 39–68.

———, 2007. Biostratgraphy and event stratigraphy in Iran around the Permian-Triassic Boundary (PTB): Implications for the cause of the PTB biotic crisis. *Global and Planetary Change*, 55: 155-176.

KOZUR, H. W. and PJATAKOVA, M., 1976. Die conodontenart *Anchignathodus parvus* n. sp., eine wichtige Leitform der basalen Trias. *Koninklijke Nederlandse Akademie van Wetenschappen (Series B)*, 79: 123–127.

KOZUR, H. W., MOSTLER, J. and RAHIMI-YAZDA, A., 1975. Beitrage zur Mikro–fauna permotriadischer schichtfolgen, teil 2, Neue conodonten aus dem Oberperm und der basalen Trias von nord- und zentral Iran. *Geologische-Palaeontologische Mitteilungen Innsbruck*, 5, no. 3, 1–23.

LEHRMANN, D. J., 1999. Early Triassic calcimicrobial mounds and biostromes of the Nanpanjiang basin, south China. *Geology*, 27: 359–362.

LEHRMANN, D. J., PAYNE, J. L., FELIX, S. V., DILLETT, P. M. and WEI, JIARONG, 2003. Permian-Triassic boundary sections from shallow-marine carbonate platform of the Nanpanjiang Basin, South China: Implications for oceanic conditions associated with end-Permian extinction and its aftermath. *Palaios*, 18: 138–152.

LINDSTROM, M., 1970. A suprageneric taxonomy of the conodonts. *Lethaia*, 3: 427–445.

MATSUDA, T., 1984. Early Triassic conodonts from Kashmir, India. Part 4, *Gondolella* and *Isarcicella. Journal of Geosciences of Osaka City University.* 24: 75–108.

MEI, S. L., 1996. Restudy of conodonts from the Permian–Triassic boundary beds at Selong and Meishan and the natural Permian–Triassic boundary. In: Wang H. Z. and Wang X. L., Eds., *Centennial memorial volume of Prof. Sun Yunzhu: Palaeontology and stratigraphy*, 141–148. Beijing: China University of Geosciences Press.

MEI, S. L., ZHANG, K. and WARDLAW, B. R., 1998. A refined succession of Changhsingian and Griesbachian neogondolellid conodonts from the Meishan section, candidate of the global stratotype section and point of the Permian-Triassic boundary, *Palaeogeography, Palaeoclimatology, Palaeoecology.* 143: 213–226.

METCALFE, I. and ISOZAKI, Y., 2009. Current perspectives on the Permian–Triassic boundary and end-Permian mass extinction: Preface. *Journal of Asian Earth Sciences,* 36: 407–412.

METCALFE, I. and NICOLL, R. S., 2007. Conodont biostratigraphic control on transitional marine to non-marine Permian-Triassic boundary sequences in Yunnnan-Guizhou, China. *Palaeogeography, Palaeoclimatology, Palaeoecology*, 252: 56–65.

METCALFE, I., NICOLL, R. S. and WARDLAW, B. R., 2007. Conodont idex fossil *Hindeodus changxingensis* Wang fingers greatest mass extinction event. *Palaeoworld*, 16: 202–207.

MUNDIL, R., LUDWING, K. R., METCALFE, I. and RENNE, P. R., 2004. Age and timing of the Permian mass extinctions: U/Pb geochronology on closed-system zircons. *Science*, 305: 1760–1763.

NICOLL, R., METCALFE, I. and WANG, C.-Y., 2002. New species of the conodont genus *Hindeodus* and the conodont biostratigraphy of Permian–Triassic interval. *Journal of Asian Science*, 20: 609–631.

PAYNE, J. L., LEHRMANN, D. J., WEI, JIARONG, ORCHARD, M. J., SCHRANG, D. P. and KNOLL, A. H, 2004. Large perturbations of the carbon cycle during recovery from the end-Permian extinction. *Science*, 305: 506–509.

ORCHARD, M,. J. and KRYSTYNI, L., 1998. Conodonts of the lowermost Triassic of Spiti, and new zonation based in *Neogondolella* successions. *Rivista Italiana di Paleontologia e Stratigrafia*, 104: 341–368.

ORCHARD, M. J., NASSICHUK, W. W. and LIN, R., 1994. Conodont from the Lower Griesbachian *Otoceras latilobatum* bed of Selong, Túbet and the position of the Permian-Triassic boundary. *Canadian Society of Petroleum Geologists Memoirs*, 17: 823–843.

SHEN, J., ALGEO, T. J., HU Q., ZHANG, N., ZHOU, L., XIA, W. C. and FENG, Q. L., 2012. Negative C-isotope excursions at the Permian-Triassic boundary linked to volcanism. *Geology*, 40: 963-996.

SHEN, S. Z., CROWLEY, J. L., WANG Y. et al., 2011. Calibrating the end-Permian mass extinction. *Science,* 334: 1367–1372.

SWEET, W. C., 1970. Uppermost Permian and Lower Triassic conodonts of the Salt Range and Trans-Indus Ranges, West Pakistan. In: Kummel, B. and Teichert, C., Eds., *Stratigraphic boundary problem, Permian and Triassic of West Pakistan,* 207–275. Lawrence, KS: University of Kansas. Department of Geology Special Publication 4.

———, 1973. Conodontophorida Eichenberg. In: Teichert, C., Kummel, B. and Sweet, W. C., Eds., *Permian-Triassic strata, Kuh-e-Ali Bashi, Northwest Iran,* 423–472. Cambridge, MA: Harvard University Press. Bulletin of the Museum of Comparitive Zoology, no. 145.

———, 1988. *The Conodonta: morphology, taxonomy, paleoecology, and evolutionary history of a long-extinct animal phylum*. London: Oxford University Press. Monographs on Geology and Geophysics, no. 10, 212 pp.

TIAN, S. G., 1982. Triassic conodonts in the Tulong section from Nyalam County, Xizong, China. *Contribution to the Geology of Qinghai–Xizong (Tibet) Plateau*, 7: 153–166.

———, 1993. Evolution of conodont genera *Neogondolella*, *Hindeodus* and *Isarcicella* in northwestern Hunan, China. *Stratigraphy and Paleontology of China*, 2: 173–190.

WANG, C. Y., 1995. Conodonts of Permian-Triassic boundary beds and biostratigraphic boundary. *Acta Palaeontologica Sinica*, 34:129–151.

WANG, G. and XIA, W., 2004. Conodont zonation across Permian–Triassic boundary at the Xiakou section, Yichang city, Hubei province and its correlation with the global stratotype section and point of the PTB. *Canadian Journal of Earth Sciences*, 41: 323–330.

WANG, Z. H. and WANG, C. Y., 1981. Conodonts. In: Zhao J., Sheng I., Yao Z.. Liang X., Chen C., Rui I. and Liao Z., Eds., *The Changhsingian and Permian-Triassic boundary of South China,* 70–81. Nanjing: Nanjing Institute of Geology and Palaeontology. Bulletin 2.

WU, S., LI, Q. and WANG, W., 1988. Characteristics of stratigraphic and faunal changes near the Permo-Triassic boundary in the Huayingshan area, Sichuan Province. *Geoscience*, 2: 375–385 (In Chinese with English abstract).

XIA, W., ZHANG, N., WANG, G. and KAKUWA, Y., 2004. Pelagic radiolarian and conodont biozonation in the Permo-Triassic boundary interval and correlation to Meishan GSSP. *Micropaleontology*, 50: 27–44.

XIE, S. C., PANCOST, R. P., YIN, H., WANG, H. M. and EVERSHED, R. P., 2005.Two episodes of microbial changes associated with Permo–Triassic faunal mass extinction. *Nature*, 434: 494–497.

YIN, H. F., FEI, Q. L., LAI, X. L., BAUD, A. and TONG, J. N., 2007. The protracted Permo-Triassic crisis and multi-episode extinction around the Permian–Triassic boundary. *Global and Planetary Change*, 55: 1–20.

YIN, H. F., ZHANG, K. X., TONG, J. N., YANG, Z. Y. and WU, S. B., 2001. The Global Stratotype Section and Point (GSSP) of the Permian–Triassic boundary. *Episodes,* 24:102–114.

ZHAN, C. K. and JIANG, W. J., 1989. The Permian-Triassic boundary transitional beds in Zhongliangshan area, Chongqing City. *Regional Geology of China*, 2: 168-171 (in Chinese).

ZHANG, K. X, LAI, X, L.. DING, M. H. and LIU, J. H., 1995. Conodont sequences and its global correlation of Permian-Triassic boundary in Meishan section, Changxing, Zhejiang Province. *Earth Science (Journal of China University of Geosciences)*, 20: 669–676 (in Chinese with English abstract).

ZHANG, K. X., LAI, X. L., TONG, J. N. and JIANG, H. S. 2009. Progresses on study of conodont sequence for the GSSP section at Meishan, Changxing, Zhejiang Province, South China. *Acta Palaeontologica Sinica*, 48: 474–486 (in Chinese with English abstract).

ZHANG, K. X., TONG, J. N., SHI, G. R., LAI, X. L., YU, J. X., HE, W. H., PENG, Y. Q. and JIN, Y. L. 2007. Early Triassic conodont–palynological biostratigraphy of the Meishan D section in Changxing, Zhejiang Province, South China. *Palaeogeography Palaeoclimatology, Palaeoecology*, 252: 4–23.

ZHAO, J. K, SHEN, J. H., YAO, Z. Q., LIANG, X. L.. CHEN, C. Z., RUI, L. and LIAO, Z. G., 1981. *The Changhsingian and Permian–Triassic boundary of South China.* Nanjing: Nanjing Institute of Geology and Palaeontology. Bulletin 2, 85 pp.

ZHU, X. S., ZHANG, D. F. and ZHONG, Y. X., 1999. Discoveries of the *Clarkina* from the P/T boundary clay bed in Taojiang section in southern Jiangxi. *Journal of Jiangxi Normal University,* 23: 162–168 (in Chinese with English abstract).